Microchimica Acta (2022) 189:440
https://doi.org/10.1007/s00604-022-05510-3

REVIEW ARTICLE

Tackling the challenges of developing microneedle-based electrochemical sensors

Hilmee Abdullah[1] · Tonghathai Phairatana[1] · Itthipon Jeerapan[2,3]

Received: 19 August 2022 / Accepted: 21 September 2022 / Published online: 3 November 2022

Abstract

Microneedles provide unique advantages in biomedical areas, particularly biosensing, because of their opportunities for minimally invasive and convenient detection. This review introduces concepts of electrochemical microneedle-based sensors for minimally invasive analysis together with insights into skin compartments for designing successful microneedles. We discuss requirements for developing microneedle-based biosensors, including electrical and electrochemical behaviors of materials (such as metals, nanomaterials, and conducting polymers) which are the key factors for sensitive biosensors. We further emphasize immobilization strategies to attach biorecognition elements to electrode materials. Moreover, we detail advanced techniques that require state-of-the-art fabrications and materials to realize porous, biodegradable, and antifouling materials to enhance biosensing performances. We also emphasize studies of cytotoxicity and damage to the skin to elucidate biocompatible potentials. Furthermore, we highlight the latest advances in microneedles published from 2019 to 2022. This review also includes an overview of key remaining obstacles and opportunities where developments will push the advances continuously. The conclusion and outlook on the status of laboratory and commercial availability are added. We prospect that microneedle sensors will be integrated into a closed-loop system biodevice for diverse applications, e.g., detection and therapy.

Keywords Microneedles · Biosensors · Wearable devices · Continuous monitoring · Minimally invasive analysis · Sensing materials · Epidermal electrochemical detection

Introduction

The ability to access human bioinformation through dynamic changes of metabolites and chemicals in biofluids is of importance to the advancement of biomedicine. In particular, continuous monitoring of significant metabolites, such as glucose in severe diabetes patients [1–8] or lactate monitoring for a critical patient [9–15], is crucial because it provides beneficial data for medical personnel to make a decision and manage treatment plans in real time [16].

Several approaches have been developed to access and detect levels of biomolecules in biofluids in the last few decades [17]. The very first wave of technology involved collecting samples from patients (such as blood, cerebrospinal, fluid, and urine); the collected biosamples were then transferred to large, expensive, and complex equipment in a clinical laboratory for analysis [5]. Subsequently, the next technology has shifted to miniaturize the standard laboratory procedures into a small chip to allow investigation of the health condition at bedside, called "lab-on-a-chip" or "point-of-care" testing devices [5]. Such technologies can reduce the complexity of traditional lab experiments and provide rapid results. However, the samples including blood, plasma, and serum must be taken out of a patient's circulation system, thus creating a large barrier that hinders real-time and continuous monitoring.

✉ Itthipon Jeerapan
itthipon.j@psu.ac.th

[1] Institute of Biomedical Engineering, Department of Biomedical Sciences and Biomedical Engineering, Faculty of Medicine, Prince of Songkla University, Hat Yai, Songkhla 90110, Thailand

[2] Center of Excellence for Trace Analysis and Biosensor, Prince of Songkla University, Hat Yai, Songkhla 90110, Thailand

[3] Division of Physical Science and Center of Excellence for Innovation in Chemistry, Faculty of Science, Prince of Songkla University, Hat Yai, Songkhla 90110, Thailand

Currently, technological advancements enable the fabrication of micro- and nano-scaled objects, which microneedles have emerged. Microneedles are micron-scaled needles that have been widely exploited for two major aspects of the medical field.

First, medical treatments where microneedles are engineered to release specific substances onto the human body through the skin in different approaches. The medical treatments can include (1) vaccine injections [18, 19] that provided promising results when compared to normal injections (e.g., measles and rubella [20], influenza [21], and poliovirus vaccine [22]), (2) drug delivery [4, 23, 24] (e.g., insulin delivery), and (3) cosmetic treatments (e.g., employing hyaluronic acid [25, 26] and magnesium [27] for anti-wrinkle treatments).

Second, another intriguing benefit of the microneedle is diagnostic biosensing [4, 23, 24]. Researchers have expressed interest in electrochemical microneedle-based biosensors because these needles can detect target analytes in dermal interstitial fluid (ISF) by directly inserting the micron-scaled sensor beneath a skin layer. Microneedles offer several advantages, such as painless insertion into the skin, causing no rash or irritation [28] and being infection-free [29]. These properties, therefore, allow the insertion of the microneedle into the epidermal surface to detect biomolecules or chemical substances continuously and in real time.

We can observe growing numbers of microneedles for biosensing applications; however, the use of a microneedle-based biosensor in medicine remains several challenges. First, physical properties involve a critical concern about the geometry of the needle, such as diameter and tip sharpness, and a distortion of the microneedle structure while inserting. Therefore, we need to reflect on the strength of the microneedle shaft and the geometry [30–35]. Second, microneedles could lead to immunological risks as the needle is penetrated the skin during detection [10, 30]. Third, for the suitable electrode, microneedle modification can be utilized to improve electric and electrochemical properties, while immobilization is also necessary to increase specificity.

This review describes the concept of a microneedle-based biosensor for minimally invasive detection in ISF as shown in Fig. 1A. It also includes key considerations of (1) geometrical designs that enhance biosensing performances, (2) mechanical properties to avoid unintentional penetrating failure, and (3) electrochemical properties to be employed for biosensors. Furthermore, we discuss challenges pertaining to the advanced techniques and materials for enhancing biosensor performances, such as fabrication techniques to obtain porous microneedles, advanced biodegradable materials to protect biorecognition layers, as well as anti-fouling agents. We highlight representative research papers that illustrate the utilization of microneedle-based biosensors to detect (1) metabolites, e.g., glucose and lactate, (2) early stage of cancer, and (3) drugs or chemical substances in the ISF or the human skin. These studies are mainly original research articles published from 2019 to now, representing a fascinating insight into the research field.

Concepts of electrochemical microneedle-based sensors for minimally invasive analysis

The term "microneedle-based biosensor" is used to describe a medical analytical tool with a thin and sharp tip that can detect and report the level of an analyte of interest in biofluids available under the human skin. The concept of using a microneedle-based sensor is to insert the needle which integrates a sensing function through the outermost layer of the dermal to access a biofluid flowing beneath our skin [2, 9, 36, 37] (Fig. 1A). Therefore, the microneedle's tip is designed to be strong enough to pierce through the stiffest layer of the outermost layer of the skin (stratum corneum) in order to reach the dermal layer, which carries full of analytes. The dermal layer consists of 5% volume of blood [38] and about 45% volume of interstitial fluid (ISF) [36]. It is noted that the ISF is mostly found in the dermis layer [39]. Intriguingly, the ISF carries rich biochemical information, such as dynamic metabolic activities. For example, the glucose level in ISF is very related to blood in a stable stage [36, 38], despite the lagging time for about 4–10 min delay [36], while the protein composition is 93% matches as in the serum and blood [36], Therefore, ISF has gained tremendous attention for under skin detection.

Electrochemical detection is one of the simplest analytical approaches, providing both quantitative and qualitative information [4, 36, 37]. It is usually a low-cost, rapid, and portable device that requires no expert to be used. The basic principle of the electrochemical biosensor is based on reactions or interactions between the biorecognition elements (such as enzyme, DNA, and antibody) and a specific analyte. Consequently, the products of the reaction/interaction from the analytes and biorecognition elements provide or use electrons which are detected by a transducer—the electrode converting one form of bio/chemical energy into another such as electricity and voltage—that is fabricated by different materials (e.g., metals or conductive polymers) as shown in Fig. 1B. The signals detected by the transducer can proceed with different techniques (such as amperometry, cyclic voltammetry, electrochemical impedance spectroscopy, and differential pulse voltammetry; Fig. 1C) and display in a friendly way.

Although the micron-sized structure of a microneedle-based biosensor limits pain and provides a noninvasive feature, the tip of the microneedle is required to insert into

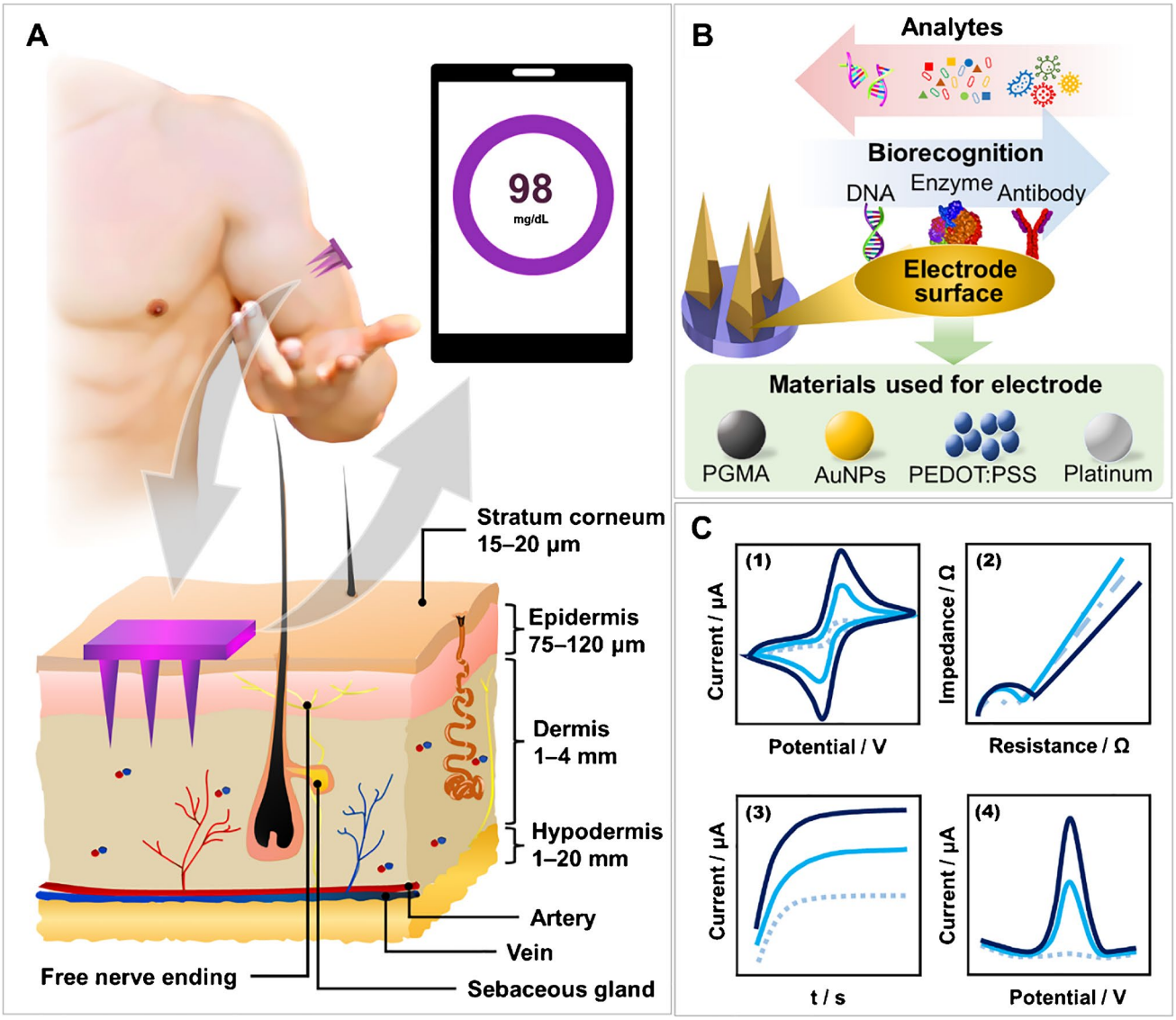

Fig. 1 Microneedle-based electrochemical sensors for minimally invasive monitoring. **A** A transdermal microneedle sensor penetrating the skin. The zoom-in image shows dermal layers. **B** The principle of a microneedle-based electrochemical biosensor. PGMA, AuNPs, and PEDOT:PSS stand for poly(glycidyl methacrylate), gold nanoparticles, and poly(3,4-ethylenedioxythiophene):poly(styrenesulfonate). **C** Electroanalytical signals obtained from different electrochemical techniques including (1) cyclic voltammetry, (2) electrochemical impedance spectroscopy, (3) amperometry, and (4) differential pulse voltammetry

the skin. The materials used to fabricate microneedles and strategies to prepare microneedle-based sensors are carefully considered (Fig. 2). The basic requirements of the materials in terms of microneedle features include (1) dimensions that can affect the pain and the performance to access the target analyte in the human biofluids, (2) mechanical properties to avoid any unexpected cracking of the microneedle, and (3) biocompatibility for cell friendly ecosystem to reduce immunological risks that may cause. The requirement in terms of biosensors includes (1) electrical and electrochemical behaviors to transduce the chemical signal to quantifiable signals, (2) biorecognition element to specify the biosensor function, (3) biodegradable, porosity, and antifouling to enhance electrochemical performances such as sensitivity and selectivity.

Considerations when developing wearable microneedle-based electrochemical sensors

Geometry

Many designs and shapes of microneedle-based biosensors have been fabricated to pierce through the skin layers and

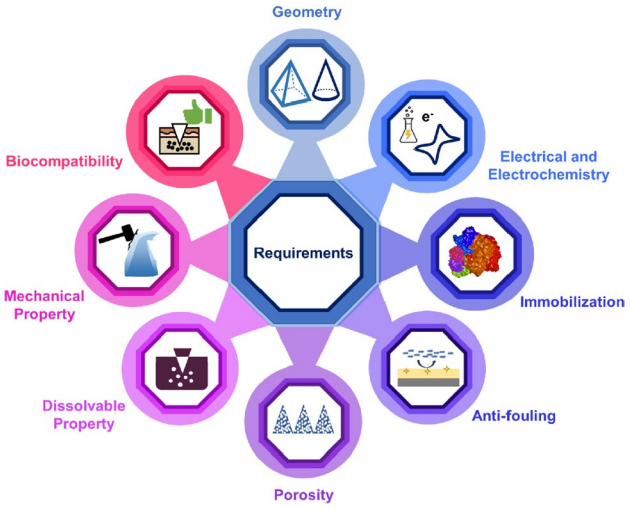

Fig. 2 Basic requirements and potential strategies to improve microneedle biosensor performances

perform electrochemical biosensors. Different geometries of the microneedle offer different features.

The primary consideration for designing the microneedle-based biosensor is the location of the analyte which we require to reach and detect. As briefly mentioned earlier in "Concepts of electrochemical microneedle-based sensors for minimally invasive analysis," the ISF is a common source of the analyte among the biofluids in the dermis. To access the ISF, the working area of the microneedle is required to be the place where the ISF resides. Hence, an understanding of skin anatomy is mandatory.

Skin compartments comprise three main layers: (1) epidermis, (2) dermis, and (3) hypodermis or subcutaneous tissue. The outermost layer of skin is the stratum corneum, which protects an interchanging between body fluid and foreign matters (such as harmful chemicals, and bacteria) [37]. The stratum corneum also prevents the loss of liquid from the body with its hydrophobic nature [37]. The thickness of the stratum corneum is about 10–40 µm [36], while the rest of the epidermis is around 75–150 µm depth [37, 40, 41] and up to 600 µm on palms and soles [42, 43]. The dermis layer is beneath the epidermis and is normally 1000–2000 µm thick but can reach up to 4000 µm on the adult back skin [36–38, 42]. From all layers of skin compartments, the interstitial fluid (ISF) is found at around 45% [36–38, 42] while the blood available is only 5%. The ISF is found mainly in the dermis than in hypodermis and can also be found in serum or cell materials. ISF resides in the interstitium which is the space between cells and vessels. The interstitium is composed of collagen, glycosaminoglycan, and elastin [38].

Sharpness is another key requirement to be carefully engineered because the needle must pierce the human skin, which is protected by the hard stratum corneum [12, 44–46]. The sharpness is described by the tip angle or radius, which can also be determined by the thickness or the aspect ratio. The penetration capability of a microneedle depends on the sharpness of the needle. Previous studies showed that the force at an initial drop to insert microneedle with tip radius between 5 and 37 µm linearly increased from 20 to 167 mN [47]. Additionally, the force at the initial drop of microneedle with a tip radius larger than 80 µm increased exponentially [48].

In addition, an aspect ratio is a proportional relationship between a microneedle's width and height, indicating microneedle integrity. The lower the aspect ratio (e.g., a small height and a large diameter of the needle base), the greater the stiffness of the microneedle obtained. However, a small aspect ratio has a trade-off because a small aspect ratio decreases the sharpness of the microneedle. Thus, these parameters should be optimized. For instance, a study demonstrated that the optimal aspect ratio is 12:1 for the material with 3 GPa of Young's modulus [49].

One of the ultimate features of microneedle-based biosensors is minimizing pain [50–52] during the penetration of the needle to lessen anxiety and a phobia about using the needle [53]. Two major factors affecting pain experiences while inserting the needle into the skin are microneedle length [53] and number [54]. The correlation between length and pain of microneedle is demonstrated. A study examined the pain score when inserting microneedles with three distinct microneedle lengths: 1000, 1500, and 2000 µm. The pain scores range from 0 to 10, where 0 represents no pain and 10 represents the highest pain level. The study found that the insertion of 1000-µm-length microneedle showed no pain, while the pain scores of 0.21 ± 0.49 and 0.71 ± 1.11 were obtained from longer needles (i.e., 1500-µm and 2000-µm needles, respectively) [53]. Another study revealed that 30% of volunteers reported painlessness when using 490-µm and 700-µm microneedles, whereas only 10% reported painlessness when using a 1490-µm microneedle. The study concluded that when increasing threefold of microneedle length, the pain score would be increased by sevenfold [55]. In addition, the pain of microneedle insertion was increased 2.5-fold while the number of microneedles was increased tenfold [55]. Other factors such as thickness, tip angle, and aspect ratio did not result in a significant increase in pain [55]. Special designs for the microneedle are introduced to enhance the microneedle's ability. Commonly, the surface of the microneedle is designed to be flat and smooth. Therefore, when applying a microneedle to the real living sample, a constant force is required to press the microneedle to fix the microneedle position. A special architecture of a spike microneedle has recently been introduced to overcome this

limitation. An example of a microneedle is printed by 3D printing technology, where some barbs (points backward from the main tip) are added at the top of its shaft. When inserting this needle, the barb helps to fix the microneedle to a steady position (Fig. 3A) [56]. Furthermore, tiny drop-liked nodes inspired by a bug scent organ were added onto the microneedle surface to expand the area and increase the liquid flow on the microneedle's surface (Fig. 3B) [57]. Figure 3C shows the microneedles with hollow [58] which can offer various purposes, such as being a microfluidic channel, loading drugs [59–61], and as holding electrode materials [62, 63]. Magnetorheological drawing lithography (MRDL) offers a promising method to fabricate microneedles for biosensors. In brief, curable magnetorheological fluid (CMRF) can be dropped on the substrate, and the magnetic field is then assisted to draw the droplet into the desired shape of the microneedle, as shown in Fig. 3D.

Mechanical properties

A microneedle-based biosensor typically accesses the interstitial fluid which is found at the epidermis and dermis layers of human skin by penetrating the stratum corneum layer. Mechanical properties are important when engineering electrochemical sensing systems for on-body applications [66]. The stiffness of the microneedle-based biosensor is carefully designed based on skin mechanical properties to ensure no breaking of microneedle during the detection. Human skin possesses several important mechanical properties which vary from different factors such as age, gender, and area of the body [67, 68]. Viscoelasticity is another essential property that provides the elongation of the skin stretching range to prevent injuries or damage when forces are applied to the skin [69]. The viscoelasticity of skin offers two different mechanical behaviors, including viscosity and elasticity at the same time.

To measure skin mechanical behavior, four important techniques can be employed for instance tensile testing [70], suction testing [71], torsion testing [72, 73], and indentation testing [68, 74, 75]. The indentation testing is essential for microneedle penetration testing as this characterization way measures a force that is applied onto a small area of skin vertically [76].

Several studies about indentation testing of microneedles have been investigated to predict the insertion force (determining a force required to break the skin) [32, 48, 77]. The demonstration of skin displacement and the insertion force behavior are reported [32, 48, 77]. Figure 4A displays a graph showing the relationship between the displacement used to insert the microneedle (that has a design with a

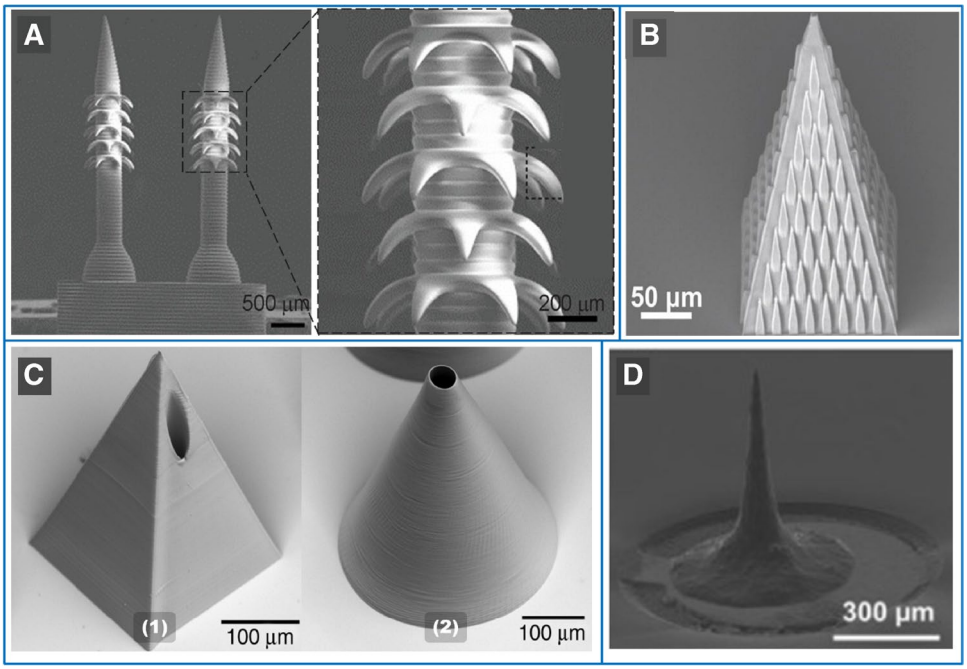

Fig. 3 Geometrical designs of microneedles. **A** The SEM images of microneedles with lateral spines. Adapted with permission [64]. Copyright 2020, *WILEY–VCH Verlag GmbH & Co. KGaA, Weinheim*. **B** Drop-liked nodes on a microneedle surface bioinspired by a scent organ of European bugs. Adapted under the terms and conditions of the CC-BY [57]. Copyright 2019, Cristina Plamadeala et al., published by *Springer Nature*. **C** Hollow microneedle designs with (1) pyramidal and (2) cone shapes. Adapted under the terms and conditions of the CC-BY [58]. Copyright 2019, Anika Trautmann et al., published by *Springer Nature*. **D** A sharp microneedle fabricated by using magnetorheological drawing lithography (MRDL). Adapted with permission [65]. Copyright 2019, published by *Elsevier*

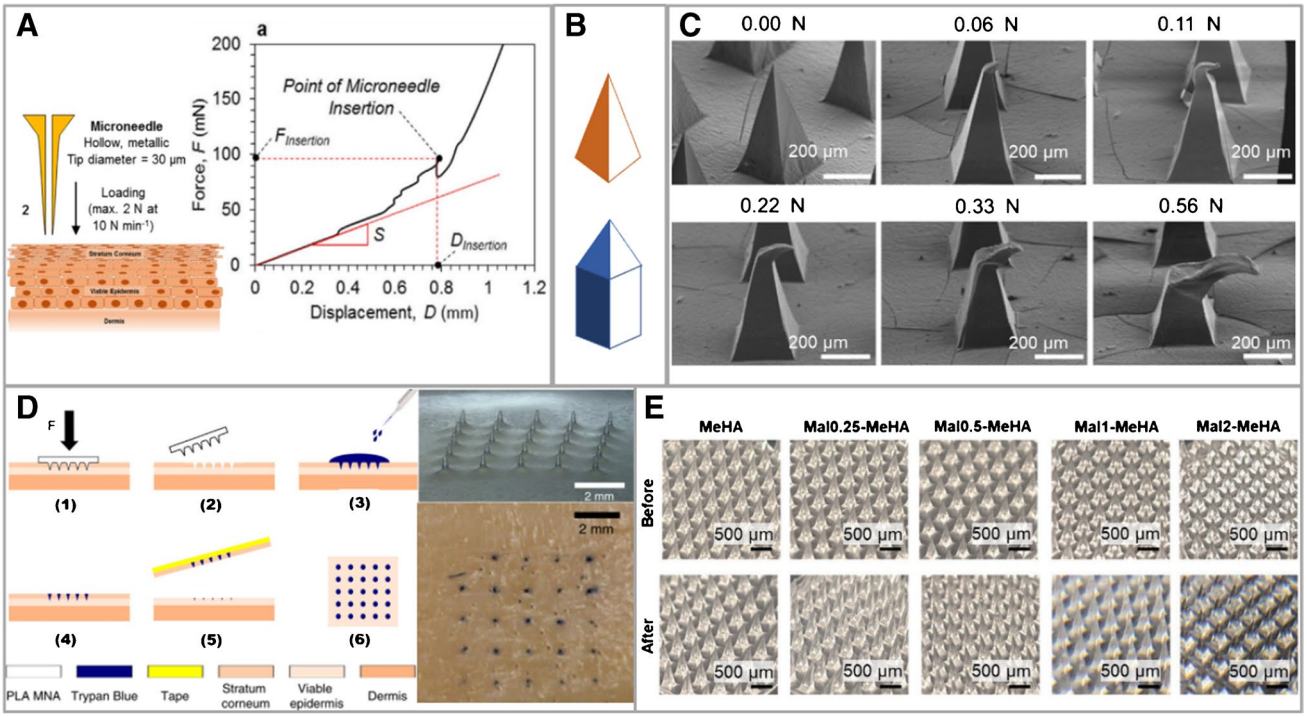

Fig. 4 Mechanical testing of microneedles. **A** (Left) Schematic of metallic hollow microneedle insertion into the skin. (Right) The graph showing the insertion force of a microneedle during penetration displaying the force required to allow the microneedle tip to pierce the skin. Adapted under the terms and conditions of the CC-BY [77]. Copyright 2016, Sahan A Ranamukhaarachchi et al., published by *Scientific Reports*. **B** (Top) Microneedle with a constant slope throughout the whole needle length and (bottom) a tip slope-shaped microneedle. **C** Microscopic images indicating a mechanical feature of polymer microneedle fabricated by spraying poly(lactic-co-glycolic acid) (PLGA) and polyvinylpyrrolidone (PVP) strength against various vertical forces, ranging from 0.00 to 0.56 N. Scale bar: 200 µm. Adapted under the terms and conditions of the CC-BY [79]. Copyright 2019, Seok Chan Park et al., published by *MDPI*. **D** Microneedle penetration testing on porcine skin using trypan blue as a marker. (Top right) The optical image of microneedles and (bottom right) the marks caused by microneedles and trypan blue. Scale bar: 2 mm. Adapted under the terms and conditions of the CC-BY [80]. Copyright 2019, Kevin J. Krieger et al., published by *Springer Nature*. (E) The optical images before and after insertion of the microneedle fabricated from composite maltose (Mal) and methacrylated hyaluronic acid (MeHA) with different concentration ratios. Scale bar: 500 µm. Adapted with permission [81]. Copyright 2020, *WILEY–VCH Verlag GmbH & Co. KGaA, Weinheim*

constant slope throughout the whole needle length as shown in Fig. 4B (top)) and the resulting force. The force–displacement plot in Fig. 4A indicates that the mechanical behavior of inserting such a needle can be divided into 3 phases. Initially, after pressing the microneedle into the skin, the resistance force gradually increases in phase 1, demonstrating the stiffness of the skin. In phase 2, the resistance rapidly decreases to a certain point when the tip of the microneedle first breaks through the stratum corneum. Consequently, the resistance rapidly increases when the microneedle is constantly penetrated further in phase 3 [77]. However, the mechanical behaviors of the microneedle with the other design (shown in Fig. 4B (bottom)) react differently. Simulation of the microneedle insertion using a finite element model demonstrates two peaks of insertion force which are responsible for tip insertion and shaft insertion respectively [78]. On the contrary, another study also measured the fracture force (a microneedle failure force) to ensure the stiffness of the microneedle, avoiding failure insertion.

Figure 4C displays the observable images obtained from the mechanical test using polymeric microneedles made of poly(lactic-co-glycolic acid) (PLGA) and polyvinylpyrrolidone (PVP) by spraying these polymers into a PDMS mold. The microscopic images show the results after the distinct force applied to the tip of the microneedle ranging from 0.06 to 0.56 N. The PLGA/PVP microneedle offers no cracking when applying vertical 0.56 N force on its tip [79].

In addition to the insertion forces and microneedle displacement, it is essential to evaluate a safety margin which is the relationship between insertion and fracture force [60]. The safety margins depend on the types and materials of the microneedle. For example, the safety margin of a solid silicon microneedle is between 6 and 9, while the polymeric hollow microneedle ranges from 5 to 20 [48, 60]. The study added that the insertion force of the microneedle increased linearly correlated with the contact area between a microneedle and skin (tip dimension). The insertion forces from the study ranged from 0.08 to 3.04 N [48], while another study

shows insertion forces of 0.104–0.111 N (human skin) and 0.083–0.118 N (porcine skin) [77].

Ex vivo insertion capability is typically confirmed using animal skin penetration testing. Porcine skin is one of the most popular models to mimic human skin, as porcine skin offers comparable mechanical behaviors. Furthermore, the freshly prepared porcine skin provides better mechanical properties than the frozen human skin [77]. Figure 4D demonstrates a skin penetration schematic on porcine skin. The microneedle is applied to the porcine skin (step 1) and removed (step 2). The trypan blue is added (step 3), followed by normal saline washing (step 4). A tape is applied to remove the stratum corneum (step 5). Eventually, the remaining trypan blue on the next layer of skin is observed (step 6) [80].

In addition to the observation of the trace left on the skin, it is essential to investigate the integrity of a microneedle. We should observe the microneedle shape before and after insertion onto the skin to confirm whether the structure of the needle integrity is suitable for penetration under expected operations. Figure 4E shows the hydrogel-based microneedle from the mixture of maltose (Mal) and methacrylated hyaluronic acid (MeHA) with different mixture w/w ratios (including 0.2:1, 0.5:1, 1:1, 2:1, and 4:1). Figure 4E shows the microneedle integrity before and after insertion into porcine skin. All mixture ratios of Mal-HeMA microneedle offer successful penetration. The 900-µm microneedles are capable to pierce to 400–500 µm depth which allows access to ISF in the dermis layer. The penetration testing of the Mal-HeMA microneedle shows no difference in the mechanical property which can be observed from the needle form after inserting [81].

Electrical and electrochemical properties when engineering microneedle-based electrodes

An electrochemical biosensor requires an electrode to serve as both a solid support as well as a transducer. The basic considerations are electrical conductivity, electron movement capacity, and potential window.

Electrical conductivity is mandatory for building electrodes to receive an effectively transferred electron from the bio/chemical reaction or interaction between biorecognition elements and target substances [82]. Electrochemical biosensors have been developed from the basic glucose sensor, which fixed the glucose oxidase (GOx) enzyme on an electrode. The biosensor should be engineered to allow high selectivity toward glucose by using a semipermeable membrane and the operation condition in the presence of oxygen. Instead of using oxygen in the original generation of the enzymatic biosensor, the mediator could be used in the second generation of the biosensor to facilitate electron transfer from the enzyme to the electrode. The third generation of the electrochemical biosensor is known as direct electron transfer (DET) [83, 84], in which the electron percolation was transferred from the biorecognition element, such as an enzyme to the electrode. However, note that there is an argument that refuses the DET behavior of glucose oxidase at some electrodes such as carbon nanotubes or graphene [85]. In many cases, the working electrode relying on conducting materials play an important role in the microneedle-based biosensor design as a transducer, as well as in determining sensitivity and selectivity [83].

A range of electrical potential without the major presence of the faradaic reaction taking place is called a "potential window" which is another important feature of material consideration. The potential window depends on the natural characteristics of materials and biofluids. The suitable potential window would allow the stability of materials and prevent material corrosion (such as in the case of metal oxidization).

Metals have been used as electrodes for decades. Cu and Ni have been employed as electrically conductive compartments due to their electrical conductivity. From the point of view of electrochemistry, Cu and Ni offer a potential window between 0.0 and 0.6 V vs SCE [86]. Metals, such as stainless steel (ferrous alloys), Ni, Ti, Pd, and Cu, were employed as microneedles [87]. However, expensive metals, such as Pt and Au, are outstanding alternative electrodes due to their wider potential windows. The window of Pt ranges approximately from − 1.0 to 1.5 V vs Ag/AgCl with a reduction peak around 0.4 V, while Au also offers a large window potential between − 0.5 and 1.7 V vs Ag/AgCl with 0.2 V reduction peak. Besides, Au is employed to fabricate electrodes in numerous studies due to its distinctive properties, such as high electrical conductivity which enhances electron transfer from biorecognition elements to electrode surface [83]. In addition, the nature of the Au surface is favorable for the immobilization of biorecognition elements (via strong thiol chemistry as discussed later in "Immobilizing biorecognition layers on microneedle-based electrodes") and maintains the element activities.

Figure 5A shows a microneedle-based biosensor that employs metals as a transducer. The 9 × 9 microneedle array is prepared. The 20-nm titanium (Ti) and 200-nm gold (Au) are consequently sputtered onto the desired surface of the microneedle array, leaving the three bared columns in the middle. The silver (Ag) is deposited on a side to serve as a precursor support for the subsequent process to fabricate a suitable AgCl surface to serve as a reference electrode. On the other side, Prussian blue covers the Au-sputtering surface to provide a sensitive layer for H_2O_2 in the glucose oxidation pathway of the biosensing mechanism. On top of that, the different types and sizes of metal provide distinct properties. Gold nanoparticles (AuNPs) are a tiny size of Au which offer a high surface-to-volume ratio and reduce the distance between the enzyme and the electrode surface.

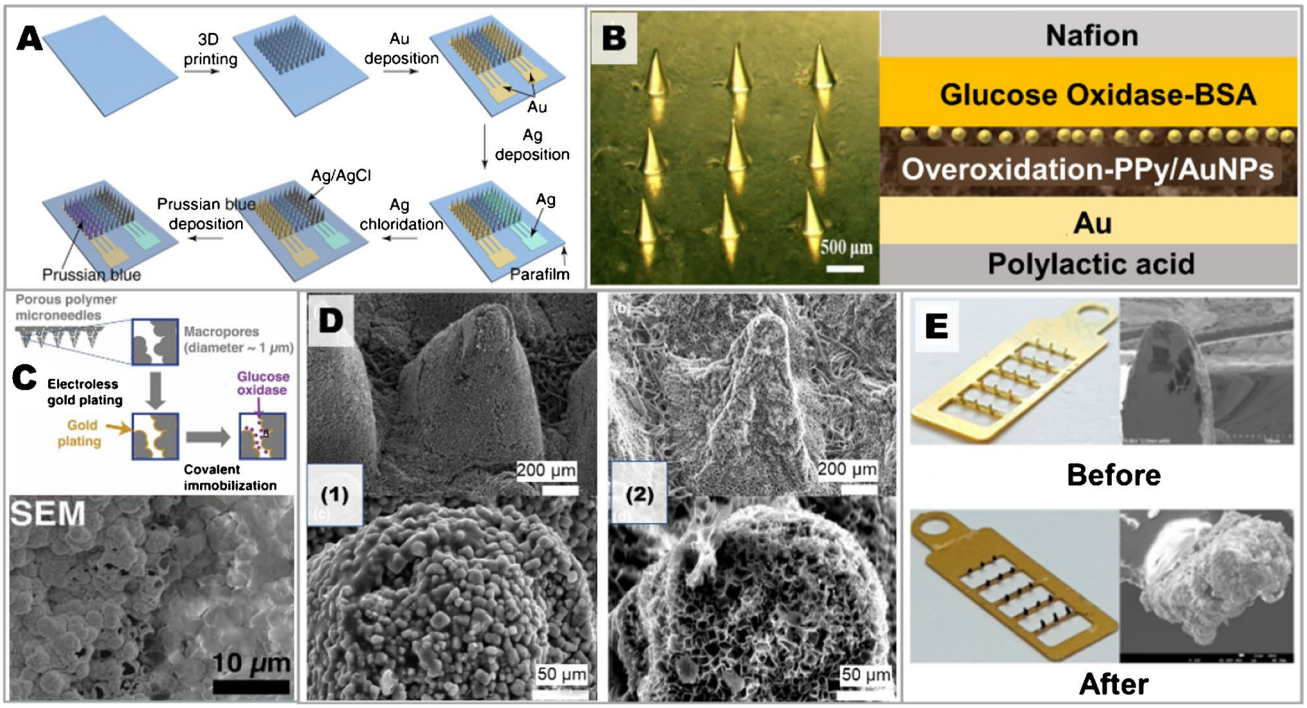

Fig. 5 Materials providing desirable electrical and electrochemical properties for microneedles. **A** 3D printing microneedles coated with Au. The arrays are divided into three different areas, including Prussian blue coated (working electrode), bare Au (counter electrode), and Ag/AgCl (reference electrode). Adapted under the terms and conditions of the CC-BY [88]. Copyright 2021, Yiqun Liu et al., published by *Springer Nature*. **B** (Left) An optical image of a microneedle biosensor coated with AuNPs and (right) the schematic illustration showing layers of the microneedle-based biosensing electrode. Adapted with permission [89]. Copyright 2020, *Elsevier*. **C** Fabrication of porous microneedle-based biosensors with gold plating and an SEM image of the microneedle surface. Adapted with permission [90]. Copyright 2020, *Wiley Periodicals, Inc.* **D** SEM images of single porous PLGA microneedle before (1) and after (2) salt leaching. Adapted under the terms and conditions of the CC-BY [91]. Copyright 2020, Chinnadayyala et al., published by *Nanomaterials*. **E** (Left) Optical and (right) SEM images of Au microneedle electrodes before and after the deposition of porous platinum black. Adapted under the terms and conditions of the CC-BY [1]. Copyright 2020, Somasekhar R. Chinnadayyala and Sungbo Cho, published by *MDPI*

These properties enhance biosensing performances and electron transfer without aiding additional mediators.

Alternatively, carbon-based materials are introduced to offer a broad potential window. Examples of carbon-based materials are glassy carbon (GC) and boron-doped diamond (BDD) that display large potential windows from − 1.2 to 2.0 and − 1.3 to 2.4 V, respectively, while these electrodes present no reduction and oxidation peaks in the ranges. Many allotropes of carbon-based materials, including graphene, graphite, and carbon nanotubes, are conductive, which is useful for building electrode materials for electroanalytical applications [92–96]. These carbonaceous polymorphs also offer similar desirable properties such as biocompatibility and stiffness [97]. Of those promising potentials, carbon-based materials are employed for an electrochemical biosensor as a substrate and an electrode.

Graphene and its derivatives have been tremendously studied in electrochemical biosensors owing to their outstanding properties. They offer rapid electron transfer [98] and favorable electroanalytical performances such as sensitivity and selectivity [94, 97]. For example, the application of graphene for fabricating the human cardiac troponin I sensor can allow a low limit of detection (LoD) at 0.07 ng mL^{-1} [98]. In addition, graphene provides high stability and reproducibility. Importantly, the large surface area from the graphene nanosheet offers a good condition for the immobilization of biorecognition elements [97, 98].

Graphene possesses high electrical conductivity (10^8 S m^{-1}) [97, 99]. Graphene provides a surface area up to 2630 m^2 g^{-1} [100, 101], which is a large effective surface area for immobilization. However, unmodified graphene has no functional groups, which limits the immobilization process of attaching biorecognition elements. To overcome this limitation and add new functional groups on the carbon surface, oxidant and strong acid treating are exploited to add carboxyl and hydroxyl functional groups onto a graphene sheet. This approach converts pristine graphene into graphene oxide (GO) [95, 97, 102]. By adding such oxygen-containing functional groups onto a graphene sheet, the GO becomes hydrophilic and enhances biocompatibility potential [97, 103]; however, the electrical conductivity of the GO decreases (down to around 5.7×10^{-6} S m^{-1} [94,

95]) because of the oxygenate insulation [97]. In regards to the electric conductivity, reduced graphene oxide (rGO) is introduced, which removes some oxygenated functional groups from the GO, providing a promising high electrical conductivity (10^2–10^5 S m^{-1} [104]). Some oxygenated functional groups remain to offer immobilization potential [82, 95, 97], allowing an attachment of molecules, e.g., protein, enzyme, polymer, and DNA [105]. An rGO has been reported to be used for a microneedle-based biosensor [97]. They demonstrate as follows: a conductive metal microneedle is prepared and immersed in the GO-contained solution. The microneedle is consequently left dry. The adsorbed GO on the microneedle surface is then reduced by ascorbic acid (vitamin C); the result converts GO into rGO. By coating the rGO on the conductive metal microneedle, the sensitivity of the H_2O_2 sensor increases [97].

Although the variety of potentials of graphene and its derivatives, the application faces challenges on various fronts. The drawbacks are that the synthesis method of graphene has no gold standard to control its size and layer, and some defections from the synthesis are still observed [94, 106].

Conductive polymers have attracted enormous interest in biosensor applications. In comparison to conventional metals, conductive polymers provide favorable properties, such as ease of processing, printing availability [82], and stability in the air that prevents forming of an insulating oxide layer [106]. On top of that, the chemical structure of conductive polymers as an electrode produces specific catalytic sites that improve electrocatalytic reactions, such as O_2 reduction [106]. Furthermore, conductive polymers' capabilities enhance many properties of biosensors. For example, they can act as the supporting material for biomolecule immobilization to improve the selectivity of microneedle-based biosensors. Moreover, hosting biorecognition elements by using conductive polymers can ensure the stability of the sensor. Using conductive polymers can also increase charge-transferring efficiency from biochemical reactions [107], thus increasing sensitivity [11, 82]. Importantly, the biocompatibility of conductive polymers to biological molecules allows biomolecule immobilization with no activity loss as well as no harm to skin, resulting in noticeable capability for continuous monitoring of analytes or drugs in human biological fluid in vivo [108].

Interestingly, a combination of different types of materials can enhance the performance of electrodes and biosensors. Figure 5B displays the deposition layers of a microneedle-based biosensor containing the conducting layer overoxidized polypyrrole (OPPy)-AuNP layer which enhances the physical and electrochemical properties of the electrode. The Cr and Au were sputtered respectively onto the surface of the microneedle to maximize conductivity. The pristine PPy is then electrodeposited onto the conducting microneedle; subsequently, overoxidation of PPy (OPPy) is performed to offer stability and surface smoothness of PPy. The OPPy, moreover, reduces AuNPs aggregation as can be seen in the study that shows the distribution of AuNPs deposition evenly onto OPPy layer [89, 109].

Advance materials and techniques for improving biosensor performances

Porosity

The electrode with a larger surface provides a wider electroactive surface area. The large area can offer high sensitivity for biosensors. Increasing the size of the electrode could increase the area of the electrode; however, this way is not practical when we want to achieve a micron-sized microneedle. There are several strategies to overcome this limitation by using special materials such as AuNPs, MWCNTs [110], and functionalized multiwalled carbon nanotubes (f-MWCNTs) [111] which are previously mentioned in "Electrical and electrochemical properties when engineering microneedle-based electrodes." On top of that, some fabrication methods are capable to increase the surface area of microneedles by creating porous structures in the microneedle's body [1, 90, 91, 98, 112, 113]. As shown in Fig. 5C, a porous microneedle was fabricated using a particle leaching method. The microneedle structure was prepared by using the monomer (i.e., glycidyl methacrylate (GMA)) and the crosslinkers (i.e., trimethylolpropane trimethacrylate (TRIM) and triethylene glycol dimethacrylate (TEGDMA)). Additionally, the porogen, i.e., polyethylene glycol (PEG) in 2-methoxyethanol, was added to the prepared polymer to create a porous in the microneedle. A photoinitiator was added to the mixture to enhance polymerization by light. The well-mixed solution was poured into the PDMS mold and exposed to UV light to cast the microneedle as shown in Fig. 5D(1). Consequently, the porogen was washed using 1:1 methanol/water. After dissolving of the porogen, the microneedle became thinner, and porous could be observed as seen in Fig. 5D(2). The Au layer was electroplated on the porous surface of the microneedle to enhance electrical conductivity [113].

Additionally, Au microneedle modified by highly nanoporous gold (h-nPG) can also increase microneedle-based biosensor performances to detect catecholamines (CAs) which is the monoamine compound of the nervous system including dopamine (DA), norepinephrine (NEP), and epinephrine (EP) [114, 115]. In brief, the 4×4 array of Au microneedles was prepared. Highly nanoporous gold (h-nPG) was then deposited on the Au microneedle surface by using a 10-mM $HAuCl_4$ solution containing 2.5 M NH_4Cl with a scan rate of 50 mV s^{-1} for 25 cycles. The potential was sweeping

between + 0.8 V and 0 V vs Ag/AgCl. Subsequently, − 2 V vs Ag/AgCl potential was applied to induce hydrogen bubbling and allow the formation of the highly nanoporous gold (h-nPG). The h-nPG-modified Au microneedle-based biosensor can detect NEP as low as 100 nM of LoD with a response time lesser than 4 s. Furthermore, the microneedle-based biosensor showed no effect from interferences including 5 mM of glucose and 500 µM of L-cysteine, L-lysine, urea, citric acid, NaCl, and folic acid [116].

Another work introduces a fabrication method to functionalize the porous platinum black (Pt-black) on the microneedle tips [1, 117]. First, the bare Au electrode was fabricated by electroplating Au onto the stainless steel support. This Au-coated stainless steel sheet was punched by using a jig and bent vertically against the substrate to create the microneedle-shaped (as shown in Fig. 5E). Before Pt deposition, the microneedle's tips and contact area were covered with PDMS and parafilm. A parylene with 5 µm thick was coated on the remaining area. Subsequently, the PDMS was removed, and microneedle tips were electrodeposited using 2.5% hydrogen hexachloroplatinate (IV) hexahydrate, lead diacetate trihydrate (0.05%), and HCl (0.01 M) in an electrochemical bath by applying a current of − 2.5 mA cm^{-2} for 400 s vs the Ag/AgCl reference electrode. This reaction allows the deposition of porous Pt black on the tip of the microneedle which can be observed as shown in Fig. 5E. The current peaks for detecting glucose obtained from bare Au microneedle vs Pt-black modified Au microneedle are significantly different. Both porous electrodes offered higher sensitivity for the detection of glucose in comparison to the smooth electrodes without porous structures.

Biodegradable materials

As mentioned earlier, microneedle-based biosensors have been developed by employing engineered materials to enhance biosensing performances. The use of metals and rigid materials is introduced to avoid fractions on the microneedle body and reduce the damage to the microneedle surface. Additionally, nanoparticles are modified on the surfaces of the microneedles to enhance electrical and electrochemical properties, while the biorecognition elements are also immobilized on the surface to increase the selectivity of analytes. However, during the insertion of microneedles into the skin, the modification layers might be mechanically damaged by the skin which could lead to a decrease in biosensor performance. Therefore, protecting the modified layer during the penetrating process could preserve the biosensing performances of the microneedle-based sensor. To overcome this obstacle, the use of dissolvable polymers is proposed [97]. For instance, dissolvable polymers, such as polysaccharide hyaluronic acid, and many polymerization degrees of poly(vinyl pyrrolidone) (PVP), could be employed owing to their biocompatible properties [118]. An example is applying PVP. First, the vertical ZnO nanowire (vNW)–coated microneedle is fabricated. Then, the dissolvable PVP solution is sprayed onto the microneedle surface and left in a vacuum to allow drying of the PVP. Upon applying the microneedle, the PVP layer could be rapidly dissolved in the ISF. A study reveals that PVP could protect the vertical ZnO nanowire (vNW) layer which is coated on the surface of stainless-steel microneedles (ssMNs) and resin microneedles (rMNs). The optical results confirm that the vNW layer remains on the surface of the microneedle after microneedle insertion. Advantageously, the PVP-coated microneedle offers 3-folded sensitivity higher than that of uncoated microneedle [119].

Antifouling materials

In the operation of microneedle-based biosensors that require in situ detection, the working electrode directly contacts the biofluid, typically ISF, where analytes are detected. Therefore, nonspecific adsorption or fouling processes might occur during operation at the working area of the electrode. Challengingly, the undesired aggregation of a foulant layer might be caused by the adsorption or polymerization of proteins, polysaccharides, and lipids as well as biomolecules (such as cells or DNA). Additionally, the fouling agent might be due to the product of a mediator [14, 120, 121]. This fouling layer obstructs electrochemical behaviors by creating an impermeable layer, which can lessen the selectivity and sensitivity of biosensor performance [14, 120, 121]. Therefore, anti-fouling agents should be included in the microneedle-based biosensor concept to maintain the signal of the microneedle-based biosensor in the presence of various interferences.

The oxidation of biomolecules at a high voltage can also generate a foulant. For example, the oxidation of NADH can form radical intermediates. Such products could alleviate the electrochemical signal by up to 70% after 1800s when using the bare carbon electrode and applying a potential of 0.75 V. However, using N-butyl-N-methyl pyrolydinium bis (trifluoromethylsulfonyl) imide (C4mpyr) (NTf2) ionic liquid (IL), MWCNTs, and the oxidation product of NAD^+ tightly attached on the carbon-based surface could reduce the signal attenuation down to 15%, owing to their ability to increase electron transfer kinetics and decrease the applied potential (down to 0.10 V) [14, 121]. The decrease of operation potential (from 0.75 to 0.10 V) could avoid the unwanted generation of radical intermediates and their dimerization during the oxidation of NADH. Therefore, this represents another example to minimize the undesired passivation on the electrode sensor, particularly for biosensors that rely on NAD^+/NADH systems (such as dehydrogenase-based enzymatic biosensors).

Additionally, antifouling agents are employed to minimize the biofouling on the microneedle surface [14, 121]. A study on development of enzymatic and nonenzymatic dual-working electrodes demonstrates the effect of Nafion coating on the stability of the microneedle-based biosensor in the presence of an ISF environment. The result showed that after 2 h of detection, the enzymatic and nonenzymatic signals decreased by 11% and 14%, respectively [122].

Immobilizing biorecognition layers on microneedle-based electrodes

In addition to the previously mentioned requirements, an electrode requires other capabilities, such as electrocatalytic activity. A crucial approach to add the desirable bioelectrocatalytic function to the microneedle is immobilizing biorecognition elements. Immobilization is a process in which biorecognition elements (such as enzymes) are fixed to or within solid supports (such as microneedle-based electrodes), thus creating a heterogeneous immobilized biorecognition element system. The immobilized form of enzymes mimics the natural mode exiting in living cells, where most of such natural catalytic systems are attached to the cellular cytoskeleton, membrane, and organelle structures.

Immobilization of biorecognition elements is one of the important parts of biosensor fabrication. Typically, oxidation or reduction reactions could occur on electrode materials when a particular potential has been applied to the electrodes. The electrochemical reaction could provide an electron transfer that could be detected at the transducer. This is important for designing electrochemical microneedle-based sensors. However, the detected signals are useful for electroanalysis only if the signals are related to a specific analyte in a biofluid that also contains other complex contaminants and admixtures. To avoid the unwanted signal from interfering species, the use of biorecognition elements is important. An enzyme is one of the most crucial recognition elements to produce a signal from the targeted analytes. In addition to enzymes, other biorecognition elements such as antibodies [123–126] and DNA [127–131] can be employed.

Additionally, enzyme immobilization provides many advantages. The solid support systems generally stabilize the structure of the enzymes and, therefore, maintain their catalytic activities. Thus, as compared to free enzymes in solution, immobilized enzymes are more robust and more resistant to environmental changes. In addition, heterogeneous immobilized enzyme systems allow the easy recovery of both enzymes and products, multiple reuses of enzymes, continuous operation of enzymatic processes, rapid termination of reactions, and a greater variety of bioreactor designs.

However, not all surfaces of the electrodes are capable of immobilizing the enzymes, and improper immobilization could also damage biorecognition molecules. Electrode's surface modification would play an important role in immobilization. Chemical modifications to add essential functional groups enhance several potentials: (1) allowing chemical bonding between the electrode surface and a biorecognition element (such as an enzyme) which increasing stability of the biosensor, (2) offering controllable orientation and density of the immobilized biorecognition element (such as an enzyme) [84, 132], and (3) preventing denaturation of a biorecognition element by adding a biocompatible intermedium layer between the transducer and the biomolecule [133].

Immobilization of biorecognition elements can be established with many methods. The simplest way is adsorption which is based on the interaction between electrode surfaces and biomolecules by weak bonds such as Van der Waal, electrostatic, and hydrophobic [134–136]. The adsorption strategy is an easy and inexpensive approach as it requires no further reagents while avoiding damage to the biomolecules. However, weak bonds provide unsteady interaction between the electrode and biomolecules which could cause leakage and denature of immobilized molecules when the environment changes [137]. Another common immobilization method uses covalent bonding which offers a strong and stable bond between an electrode surface and a biorecognition element [138, 139]. This bonding could also support self-assembling monolayer (SAM) before performing immobilization. To achieve successful covalent immobilization, a large number of molecules and many reagents are required. The activity of some biorecognition elements is also interrupted due to the newly formed covalent bonds [140]. Entrapment is another common enzyme immobilization method used for biosensors owing to their stability. The entrapment could be done by polymerization in the presence of biorecognition elements; the molecule is confined in polymer and attached to the electrode surface. This immobilization method offers strong constraining of the molecules which reduces the leaching of biorecognition elements. However, the polymers used to entrap could obstruct the molecule's activities [141].

Figure 6A shows synergistic coordinations of materials used in a microneedle-based biosensor for continuously detecting ketone bodies by the analysis of β-hydroxybutyrate (HB) and glucose. The electrode was fabricated using a combination of carbon paste, 1-ethyl-3-methylimidazolium bis(trifluoromethylsulfonyl)imide (ionic liquid, IL), and phenanthroline dione (PD) mediator. The IL used in this system assists in the adsorption of biomolecules: β-hydroxybutyrate dehydrogenase (HBD) HBD coupled with NAD^+ into the tiny pores of the underlying carbon-based electrode. The biomolecules are also crosslinked by

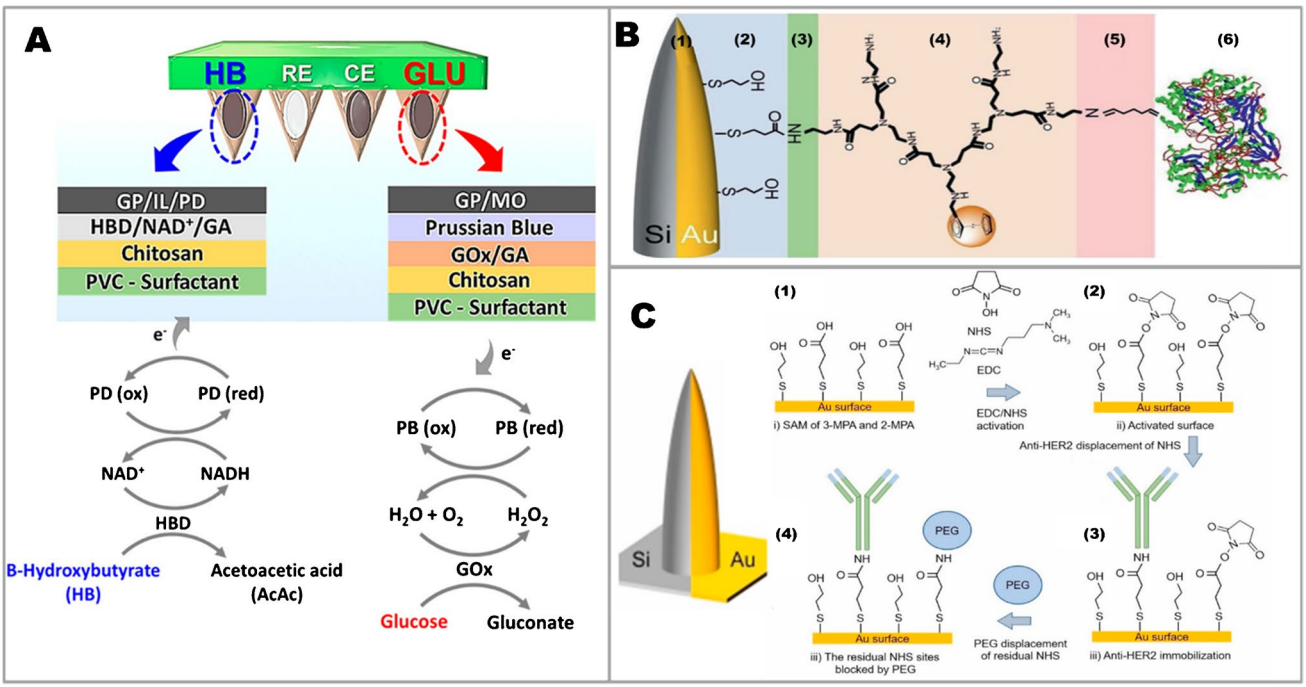

Fig. 6 Immobilization of biorecognition layers on microneedles. **A** The schematic illustration showing the immobilization of microneedles with (left) β-hydroxybutyrate dehydrogenase (HBD), nicotinamide adenine dinucleotide (NAD^+), glutaraldehyde (GA) followed by chitosan and PVC layers for the β-hydroxybutyrate (HB) sensor and (right) Prussian blue, glucose oxidase (GOx), and GA, followed by chitosan and PVC layers for glucose sensor. Adapted with permission [14]. Copyright 2019, *American Chemical Society*. **B** The schematic diagram showing immobilization of a silicon microneedle with (1) Au layer, (2) self-assembled monolayer of 3-mercaptopropionic acid and 3-mercaptoethanol, (3) activation of N-ethyl-N′-(3-(dimethylamino)propyl)carbodiimide/N-hydroxysuccinimide (EDC/NHS), (4) ferrocene-cored poly(amidoamine) (Fc-PAMAM) immobilization, (5) glutaraldehyde (GA), and (6) glucose oxidase (GOx) immobilization. Adapted with permission [142]. Copyright 2021, Wiley–VCH GmbH. Adapted with permission [142]. Copyright 2021, *Wiley–VCH GmbH*. **C** The schematic illustration showing immobilization of a microneedle using of self-assembled monolayer of 3-, and 2-mercaptopropionic acid (MPA), followed by EDC/NHS activation, anti-HER2 immobilization and PEG-diamine addition to react the excess NHS sites., respectively. Adapted with permission [143]. Copyright 2021, *Elsevier*

glutaraldehyde (GA) and coated with chitosan and polyvinyl chloride (PVC) to immobilize the microneedle [14].

Figure 6B shows the layers of covalent enzyme immobilization by using glutaraldehyde (GA) and N-ethyl-N′-(3-(dimethylamino)propyl)carbodiimide/N-hydroxysuccinimide (EDC/NHS) as crosslinker. The microneedle is first coated with Au. The –COOH functional group on the Au surface is then formed by using a self-assembled monolayer (SAM) of 3-mercaptopropionic acid. The EDC/NHS then links a bond between the carboxyl group on the activated Au and the Fc-PAMAM. GOx is then covalently bound onto the next layer of the microneedle's surface by GA crosslinking. The Fc derivative and crosslinkers in this study also act as a mediator to facilitate the electron from the active site to the transducer.

Figure 6C displays a way to attach an anti-HER2 monoclonal antibody onto the surface of a microneedle-based biosensor. This antibody contains an amino functional group that is important for covalent attachment. The formation of SAM on an Au-coated microneedle electrode is carried out by 3-mercaptopropionic acid and 2-mercaptopropionic acid. The –COOH functional group is then activated by EDC/NHS. The antibody is then covalently added to the microneedle, and the excess NHS is replaced by PEG-diamine to reduce the remaining active sites.

Concerns of toxicity and damage to the skin

Microneedle-based devices are required to be compatible with the human body [144]. According to the International Organization for Standardization (ISO) 10,993, all medical devices, especially direct-contacted instruments, are required to pass a series of biocompatible tests, such as genotoxicity, hemocompatibility, cytotoxicity, irritation, sensitization, and immunotoxicity [145], before entry to the clinical trial [145–148]. Therefore, microneedle-based biosensors are also required to be safe for users [145–148]. For instance, the insertion of the microneedle-based biosensor should not release any hazardous substances or cause any harm (such as irritation) to human skin [28], flammable [145, 147], and

immunological risk [149], to the biological environments, including cells, tissues, and biofluids [147].

Metals, such as gold, silver, titanium, and chromium, are commonly used for biosensors due to their promising electrochemical behavior and biocompatibility. Recently, conducting polymers, e.g., polyaniline (PANI), polypyrrole (PPy), and poly(3,4-ethylenedioxythiophene) (PEDOT), have been used as electrodes for biosensors, thanks to their low cost, managing simplicity, and also biocompatibility [150]. Additionally, some conducting polymers allow biomolecules to be immobilized on their surfaces without negative effects [107, 108]**.** Decreasing immunological risks while also promoting biomolecule immobilization is essential for biosensing applications.

However, before using the microneedle-based device in animal or human models, in vitro assays are typically employed for primary screening, for instances, cell viability [147], MTT assay [148], and inflammation marker [142, 148, 151, 152]. These in vitro assays, moreover, are simple and cheap ways while offering more sensitivity in comparison to a study in animal models [142, 147, 148, 151, 152].

In vitro cytotoxicity testing of the releasing agents from microneedle materials is demonstrated. The microneedles made of three different types of cyclic olefin polymers (COPs) were incubated to obtain eluates. The eluates were separately mixed with the cell medium to achieve testing media. Each testing medium was then used to incubate endothelial cells and keratinocytes at 37 °C for 24 h. Figure 7A and B show the cell viability of endothelial cells and keratinocytes, respectively. Both figures show that COPs have no effect on the cell proliferation and the medium result, whereas the control experiment (using H_2O_2) causes severe damage to the cells. Additionally, no inflammation markers including E-selectin, ICAM-1, and HLA-A/B/C were observed after 7 days of incubation [147]. Another study in Fig. 7C displays the test of cell cytotoxicity, using 3-(4,5-dimethylthiazol-2-yl)-2,5-diphenyltetrazolium bromide (MTT) assays. This assay is important to investigate the effect of the microneedle-based biosensor (made of AuNW hydrogel) on HeLa cells. The cell viability graph shows that the AuNW hydrogel microneedle-based biosensor offers good biocompatibility (cell viability over 85%) after 28 h of incubation [148].

Skin cross-sectioning and color staining are employed to ensure that a microneedle can successfully pierce skin for accessing biofluids underneath. Figure 7D shows SEM images, trypan blue staining, and cross-sectioning of piglet skin before and after microneedle penetration. Trypan blue staining obviously demonstrates the microneedle marks as the blue dots are easily observed after applying the trypan blue, whereas the cross-sectioning shows the depth of the microneedle holes caused by the penetration of the microneedle. The damage and effect of microneedles to skin are consequently confirmed after the screening tests by in vivo studies. These in vivo tests are to ensure that there will be no negative effect to patient skin. In this regard, animal models are introduced to such examinations [142, 148, 151]. Hairless mice can be employed to study the consequence of two different polymeric microneedle insertion. Microneedles are inserted into the skin for 24 h before being removed with a frequency of once a week for five consecutive weeks. The report shows that the weight of all individual mice increased throughout the experiment, elucidating a good health of mice. The microneedle marks disappeared before the next insertion. Additionally, tumor and inflammation biomarkers are not detectable in the experiment [151], indicating good biocompatible potential. Additionally, Fig. 7E shows erythema of human skin after the insertion of the microneedle for 6 h. The results show that the microneedle's mark gradually disappeared after 1 h of removal and completely disappeared after 12 h [19].

Advanced applications of microneedle-based biosensors

Monitoring metabolites

Glucose biosensors have been extensively studied over the last few decades. In fact, continuous glucose monitoring (CGM) is commercially available on the market [8, 153–155].

For managing diabetes, the vast majority of wearable biosensors rely on glucose monitoring. In addition to glucose, other biomarkers are also important to diagnose problematic situations of patients. Hyperglycemia and metabolic acidosis can be dangerous. Acidic compounds known as ketone bodies can accumulate during complicated diabetes. Life-threatening metabolic complications diabetic ketoacidosis (DKA) are interesting to be monitored by detecting the level of β-hydroxybutyrate (HB) [156–158]. In addition to detecting glucose alone, one study introduces the dual-analyte microneedle-based biosensor that can detect both levels of glucose and β-hydroxybutyrate (HB) simultaneously (Fig. 8A). The microneedle substrate in this example is fabricated by using CNC-milling technique containing two hollow microneedles for reference and counter electrodes while remaining another two for working electrodes. The first working electrode is designed for glucose detection. The glucose-sensing electrode exploits carbon paste with mineral oil for creating a transducer, followed by Prussian Blue as a mediator and the catalytic GOx layer crosslinked by glutaraldehyde (GA). The other working electrode is engineered for HB detection. The ionic liquid (IL) and phenanthroline dione (PD) mediator synergistically cooperate with carbon pasted to play as a transducer for the HB-sensing electrode.

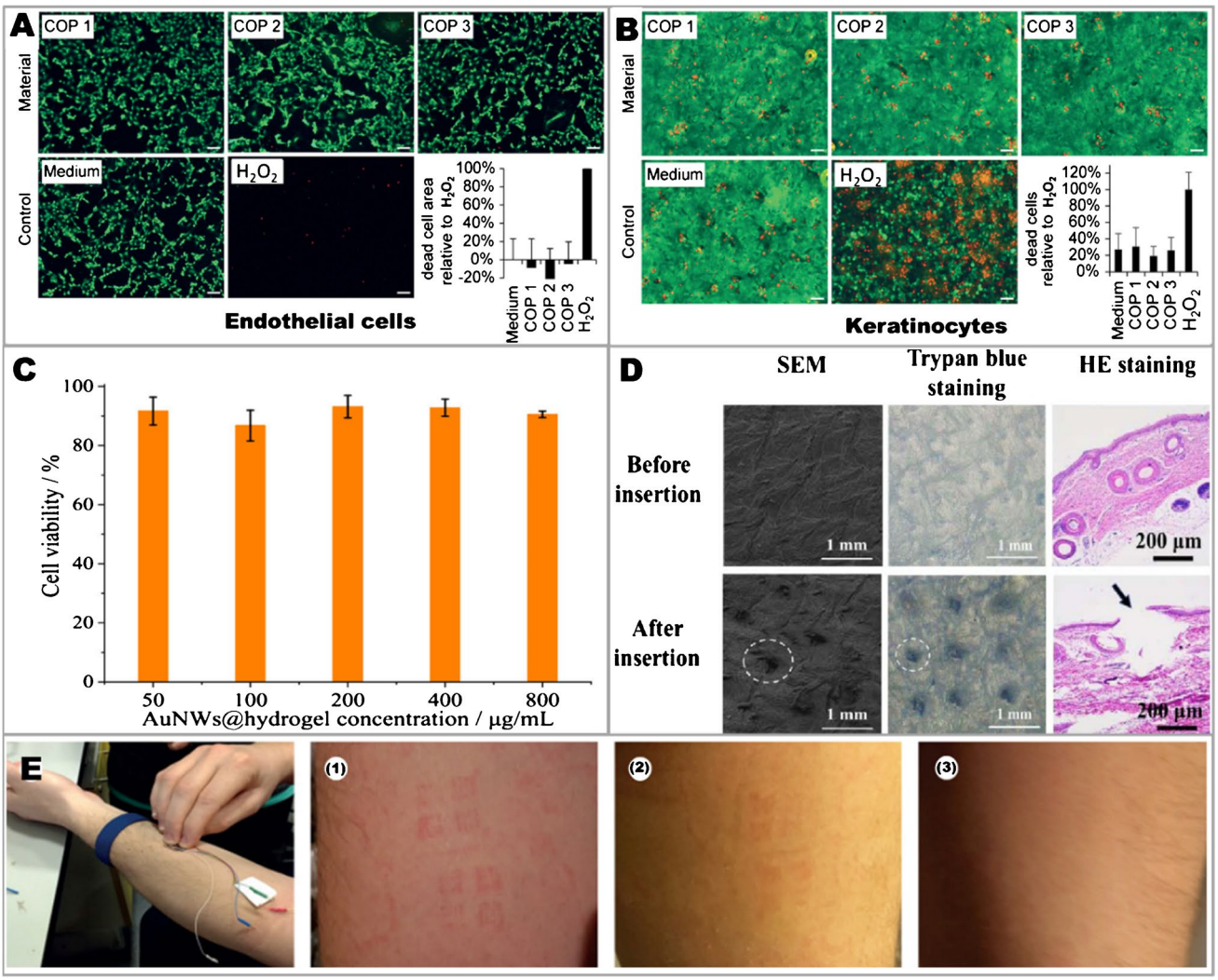

Fig. 7 The investigation of using a microneedle-based electrode in biological environments. **A**, **B** Immunofluorescent images of **A** endothelial cells and **B** keratinocytes: Live cells showed as green color (Calcein AM-stained), and dead cells showed as red color (EthD-1-stained). The upper row shows the cell viability of cells with different materials; lower row shows cell viability in control medium and H_2O_2. The graph shows the dead area of both cells with different conditions compared to H_2O_2. Adapted under the terms and conditions of the CC-BY [147]. Copyright 2019, Klaudia Schossleitner et al., published by *Wiley Periodicals, Inc.* **C** The effect of different ratios of the AuNW hydrogel microneedle on cell viability and **D** images showing piglet tissues before and after the insertion of the microneedle, trypan blue showing blue color of microneedle marks, and the H&E staining show the cells and its compartments that were applied by microneedle. Adapted with permission [148]. Copyright 2019, *American Chemical Society*. **E** Applying site of microneedle-based biosensor on human forearm and the development of mark immediately after removal, 1 and 12 h after removal. Adapted under the terms and conditions of the CC-BY [19]. Copyright 2019, Timothy M Rawson et al., published by *Elsevier*

IL used here plays roles for this biosensor: first, to constrain the biorecognition molecule by possessing tiny pores as well as to adsorb the NAD^+ with hydrogen bond; second, to increase the sensitivity for the detection of NADH. The next layer containing the biorecognition element relies on the combination of β-hydroxybutyrate dehydrogenase (HBD) and NAD^+ which were crosslinked with GA. Both working electrodes are coated with chitosan and PVC to protect the sensor from foulant agents, while the Triton X-100 serves as surfactant and avoids leaching of all functionalized layers. The detection range of HB for this microneedle-based biosensor ranges from 0.2 to 10.0 mM, which is covering the necessary range of HB detection for normal HB level (0.6–1.5 mM), high risk (1.5–3.0 mM), and critically DKA patient (> 3.0 mM). Furthermore, HB detection is highly selective against species found in the ISF, such as 200 μM for ascorbic acid (AA), uric acid (UA), and acetaminophen (AP).

Lactate is also an indicator related to cell metabolism which is useful information in an intensive care unit [159,

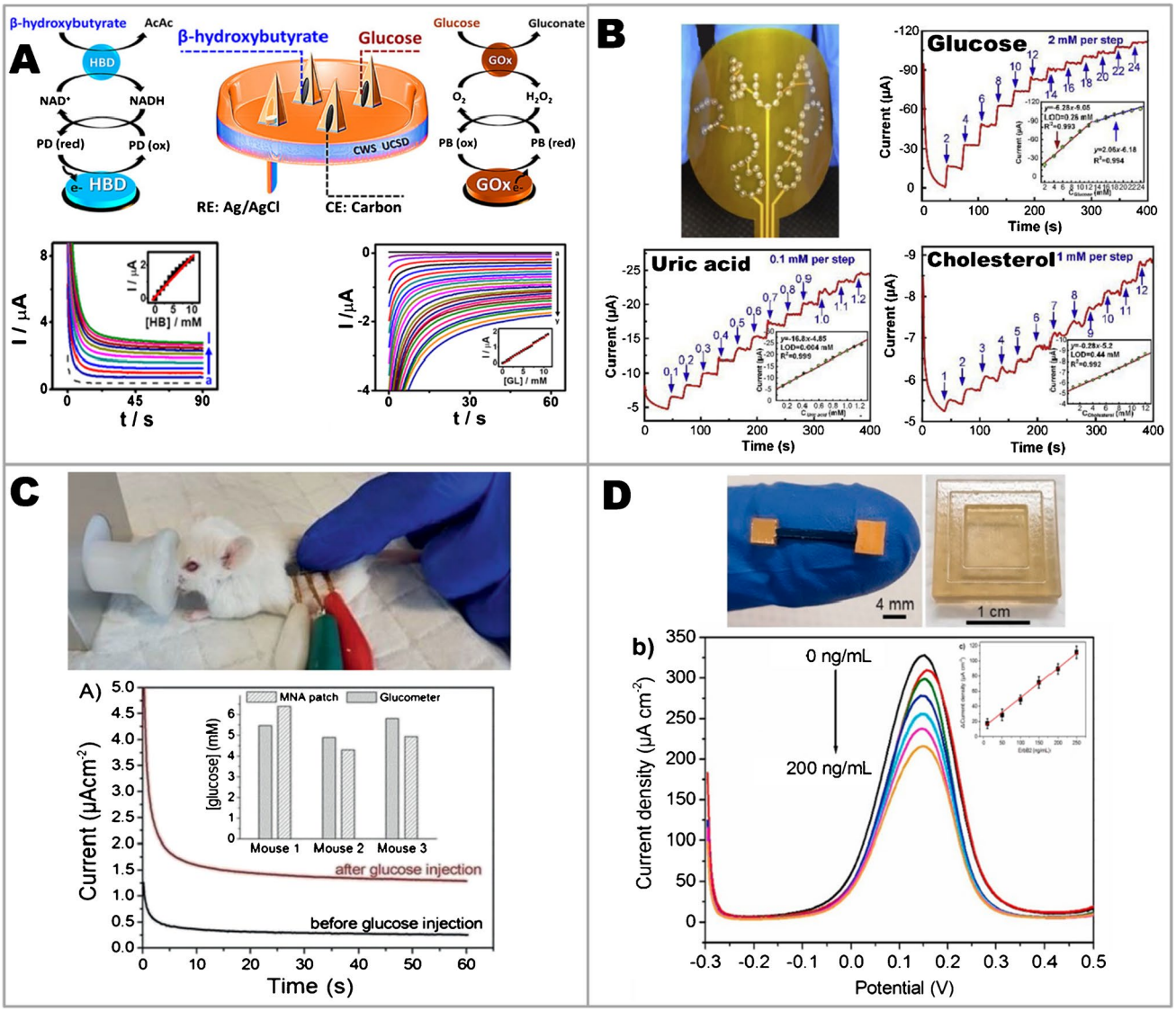

Fig. 8 Mechanisms and electrochemical signals of microneedles for measuring different analytes. **A** Carbon-pasted microneedle biosensor for HB and glucose sensors and amperograms toward monitoring HB and glucose with inset calibration curves. Adapted under the terms and conditions of the CC-BY [14]. Copyright 2020, Rupesh K. Mishra et al., published by *American Chemical Society*. **B** An optical image of a flexible microneedle-based biosensor and an amperometric graph along with inset calibration curves toward detecting glucose, uric acid, and cholesterol. Adapted with permission [65]. Copyright 2019, published by *Elsevier*. **C** The application of a microneedle biosensor onto the back of a mouse and amperometric responses of glucose before and after glucose administration by intramuscular injection. Adapted with permission [142]. Copyright 2021, *Wiley–VCH GmbH*. (D) DPV of a microneedle-based ErbB2 sensor, covering a range from 10 to 250 ng mL^{-1} with the inset calibration curve. Adapted with permission [143]. Copyright 2021, *Elsevier*

160] and sport activity [161–163]. Microneedle-based biosensors for lactate detection have been widely studied recently. One example of a microneedle-based biosensor for simultaneously detecting glucose and lactate is developed by using a solid substrate microneedle coated with different layers [10]. The microneedle substrate is fabricated using an injection molding technique to obtain four arrays of 4 × 4 microneedles, including two working electrodes for glucose and lactate separately and counter and reference electrodes. Both working electrodes are coated with Au, followed by Au-MWCNTs electrodeposition, and methylene blue is subsequently electropolymerized. Afterward, working electrodes are functionalized with enzymes for recognition events. The glucose biosensor is modified by FAD-glucose dehydrogenase (FADGDH), and the lactate working electrode is functionalized by lactate oxidase (LOx) by drop casting method. This dual-analyte detection system offers 0.05–5.0 mM and 0.01–0.1 mM linear ranges for glucose and lactate detection, respectively. The sensitivity of glucose detection is around

405.2 mA cm^{-2} mM^{-1} and the sensitivity of lactate detection is around 797.4 mA cm^{-2} mM^{-1} [10].

An example of multianalytes detecting microneedle-based biosensor is shown in Fig. 8B. Three arrays of flexible microneedle electrode array-based biosensor (MEAB) are fabricated each array for different analytes, including glucose, uric acid, and cholesterol which provide linear ranges of 2.0–12, 0.1–1.2, and 1.0–12 mM, respectively [65]. Figure 8C-top shows in vivo detecting of glucose in an alive mouse. The mouse was shaved on its back, and the microneedle-based biosensor was applied. The result shows different current responses before and after injection of glucose as shown in Fig. 8C-bottom; intriguingly, the glucose response time was less than a minute. This in-vivo experiment with promising response time is a good step in microneedle-based biosensor development [142].

Another integrated sensor for measuring pH, nitrate, and phosphate in one microneedle-based device was prepared by modifying hypodermic needles. The needle was coated with carbon nanotube/cellulose nanocrystal (CNT)/CNC), followed by silver nanoparticles (AgNPs) to obtain a nitrate sensor (LoD 0.008 mM nitrate). Additionally, the polyaniline (PANI) was coated to achieve pH measurement (linear range covering pH 3–10), and ammonium molybdenum tetrahydrate (AMT) was modified to create the sensor for phosphate detection (LoD 0.007 mM) [164].

On-body performances using a microneedle-based biosensor have been examined. Another example of a microneedle sensor composed of a reusable electronic system and a disposable microneedle, which were integrated into a portable device to detect metabolites such as glucose, lactate, and alcohol [13]. This system of a microneedle-based biosensor was engineered to be continuously monitored on a smartphone through mobile application wirelessly. In this work, the participants were advised to perform different tasks (such as doing exercise, consuming food, and drinking alcohol) to measure different metabolites. To measure lactate, the participants were asked to do an exercise. The result showed that moderate-intensity of exercise the lactate was increasing from the resting state (1–2 mM lactate) without reaching the peak, while after 4 min of high-intense exercise, the lactate level reached the peak (11.8–18.1 mM lactate) and moderately declined to the resting state. Glucose concentration was monitored while assigning the participants to eat a meal. The glucose signals rose to the peak after eating meal for some period and then gradually declined to the resting state. Alcohol monitoring could also provide continuous monitoring in real-time. The alcohol reached its peak at 0.012 to 0.034% or (2.6–7.4 mM). Interestingly, the dual-analyte detection sensors could be performed simultaneously. In order to detect alcohol and glucose simultaneously, alcohol and glucose sensors were integrated on the same microneedle patch. At the early time of the experiment, the participants were asked to drink alcohol. The alcohol signal rose to its peak and declined moderately, while the glucose signal was steady. Once the human subject took a glucose-rich meal, the glucose signal increased to the peak and gradually declined, while the alcohol signal was steady. Similarly, the dual-analyte lactate-glucose sensor was also tested. The human subject was asked to do exercise with high-intensity and eat glucose-rich meal after a period. After exercising for 4 min, lactate levels reached their peak and declined, while glucose levels reached their peak after eating. The results from alcohol-glucose and lactate-glucose showed no interferences of detecting two analytes continuously.

Early diagnosing cancer

Apart from the metabolite measurement, electrochemical techniques can be employed for early diagnosis of diseases with high sensitivity, such as cancer [143, 165–168], melanoma cancer [169], and an infectious disease involving HIV-related DNA [170]. Microneedle-based biosensors have been developed for early detection of cancer and some other biomarkers such as levodopa [122], cystatin C [171], K^+ [172], and β-lactam antibiotics [173].

One example of an electrochemical immunosensor for breast cancer is proposed as a demonstration for early diagnosis of cancer by microneedle-based biosensor. The breast cancer detection system relying on a microneedle-based biosensor is designed to detect human epidermal growth factor receptor 2 (ErbB2, also called HER2) level, the important biomarker for breast cancer, that is bound with anti-HER2. The microneedle is fabricated by using a silicon substrate coated with Au as a transducer. The Au is activated by EDC/NHS followed by anti-HER2 antibody. The breast cancer microneedle exploits differential pulse voltammetry (DPV) to detect the different concentrations of ErbB2. The microneedle offers detection of ErbB2 between 10 and 250 ng mL^{-1} range in artificial ISF while providing 50–250 ng mL^{-1} in the phantom gel (a mimic skin layer) (Fig. 8D). The LoD of the microneedle tested in artificial ISF and phantom gel is 4.8 ng mL^{-1} and 25 ng mL^{-1}, respectively. On top of that, with the antibody-antigen principle, the microneedle can capture the biomarker as well as performing electrochemical detection simultaneously.

Another example of cancer screening using microneedle-based technology is microneedle for melanoma detection. This biosensor is designed to detect tyrosinase (TYR) enzyme which is one of the most important biomarkers for screening melanoma cancer. The TYR is detected indirectly using the catechol (CAT) oxidation; catechol, which is immobilized onto the detection area, is oxidized by TYR to benzoquinone (BQ). Consequently, the BQ concentration is measured by using an amperometry technique. Hence, the

TYR level could be implied according to the corresponding signal of BQ. This sensor exploited a hollow microneedle. The CAT-filled agar is functionalizing onto the carbon paste electrode surface that is packed into the hollow for microneedle electrode. This biosensor provides the detection of TYR on both surface and beneath the skin layers [169].

The detection of drugs and toxic substances

Using a microneedle-based biosensor is a technology that has also been exploited for detecting drugs and toxic substances, such as fentanyl, opioid [174], and levodopa (L-Dopa) [63, 122]. Fentanyl is one of the synthetic opioids that has been used for pain relieving drug. Overintaking of this drug can lead to drug addiction and cause serious mortality effects [175, 176]. However, the symptoms of opioid overdose and nerve agent poisoning are difficult to be differentiated because of their similarity. A concept to leverage a microneedle-based biosensor to provide information about fentanyl and opioid level has been introduced as shown in Fig. 9A. Four microneedles with hollow structures to allow the packing of the electrode material for the detection of such analytes are fabricated for the integrated sensing system containing two working electrodes. The first working electrode is a nonenzymatic biosensor that is packed with carbon paste. This nonenzymatic electrode to detect fentanyl using a square-wave voltammetric (CSWV) technique provides a linear range from 10 to 200 µM. Simultaneously, the first working electrode can also detect morphine over a range of 20 – 140 µM. The second working electrode relies on an enzymatic recognition layer which immobilizes organophosphorus hydrolase (OPH) coated with Nafion on the carbon paste transducer. This enzymatic microneedle-based biosensor can detect organophosphate (OP) nerve agents over a range of 10 – 160 µM, with LoD of 10 µM. In addition, to achieve a low LoD of OP nerve agents, the researchers also used the combination of carbon paste and CNT on the first layer, followed by AuNPs, and rGO respectively as a transducer. With this electrode, the LoD of OP nerve agents can be lowered down to 50 nM.

Another example of a microneedle-based biosensor for continuous monitoring of drug levels is L-Dopa biosensor. L-Dopa is a precursor to dopamine [177–179]. The L-Dopa has been recognized as a gold standard for the patient with Parkinson's disease (PD) treatment [178]. The dose of L-Dopa treatment can vary, depending on the progress of the disease [23, 180]. However, diagnosing a disease by only observing symptoms can be difficult and inaccurate. In this regard, a group of researchers introduces a microneedle-based biosensor using electrochemical techniques to analyze

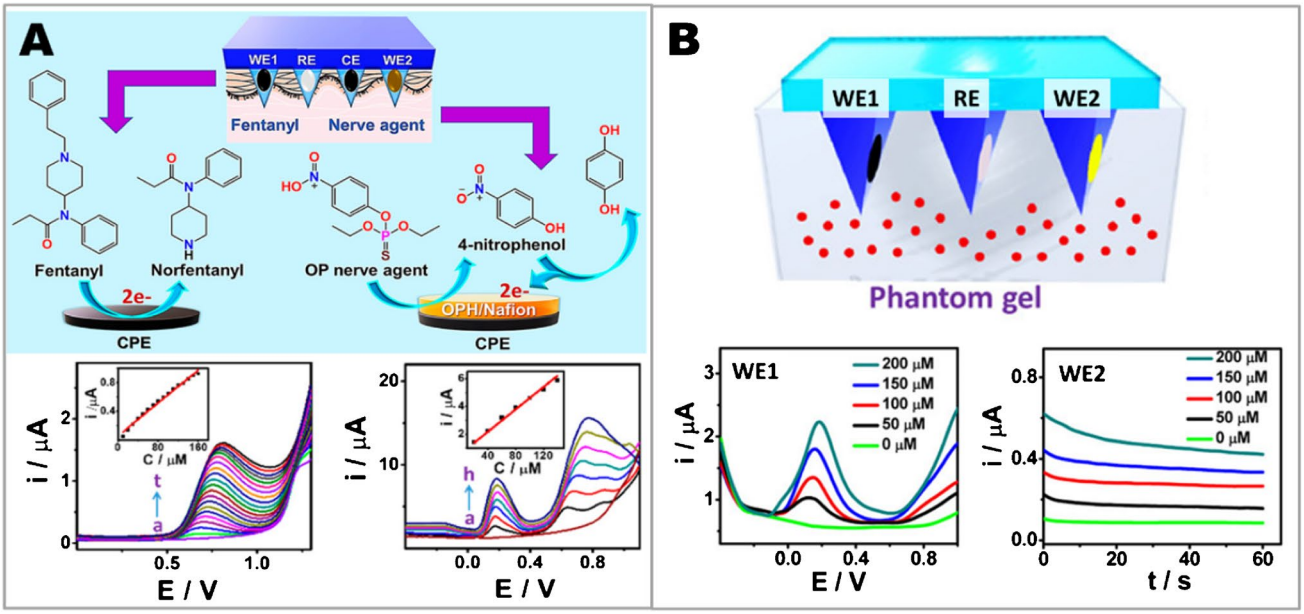

Fig. 9 Schematic illustrations and electrochemical signals of microneedle for determining drugs and toxic substances. **A** Mechanisms to monitor fentanyl and a nerve agent by using carbon-pasted microneedles. Square wave voltammetric (SWV) curves of fentanyl with the inset calibration curve over 10–200 µM range (oxidation peak is observed at 0.7 V) and CV of morphine with various concentrations over 20–140 µM range; the inset calibration curve of morphine shows oxidation peak at 0.2 V. Adapted with permission [174]. Copyright 2020, *American Chemical Society*. **B** Hollow microneedles for L-Dopa detection in phantom gel. SWV in the scan potential between – 0.4 and 1.0 V (WE1), and amperometric perform at – 0.6 V vs Ag/AgCl reference electrode (WE2) to detect L-Dopa in different concentrations ranging from 50 to 250 µM with 50 µM increment. Adapted with permission [122]. Copyright 2019, *American Chemical Society*

the concentration of L-Dopa. The first working (WE1) electrode contains non-functionalized carbon paste coated with Nafion, as a transducer. Square-wave voltammetry (SWV) was carried out to detect L-Dopa on this site. The second working electrode (WE2) uses the Nafion-coated tyrosinase-modified carbon paste employing chronoamperometric technique Fig. 9B. This microneedle-based biosensor offers good performances of the L-Dopa biosensor such as high sensitivity, good stability, and biocompatibility. The combination of dual-sensing in one microneedle-based biosensor, performing in skin mimicking phantom gel, shows a wide range detection of L-Dopa concentration, i.e., between 50 and 250 μM, whereas up to 360 μM, when performs in artificial ISF [122]. This advanced system can play an important role in biosensing part of wearable devices in the near future [181].

Conclusions and perspectives

A microneedle-based biosensor is an intriguing and useful technology in biomedical and sport fields. The tiny size of a microneedle offers unique potential for biosensing devices, such as painless and minimally invasive. Interestingly, the on-body detection basis of using the microneedle-based biosensor could break through the barrier of conventional discontinuous one-time detection into continuously monitoring. Despite many studies having been published, very few microneedle-based biosensors have been commercially available due to some limitations. For instance, a primary concern is pertaining to mechanical properties of the microneedle while inserting the sensor. Many materials are carefully recruited to provide a strong microneedle. Some materials (e.g., PLA, polycarbonate, and biocompatible polymer) are used as a substrate, while others (e.g., metals and conductive polymers) can be used as both substrate and conducting materials.

Although the geometrical surface of a microneedle is larger than the flat surface electrode, the net active area of the microneedle is very limited. Various studies employ special materials such as nanomaterials [182, 183] or develop outstanding methods, for example, adding porosity to increase the surface area or roughness of the microneedle-based electrode for enhancing biosensor sensitivity. Utilizing dissolvable polymers could protect the working area of the microneedle, which increases stability and sensitivity of the biosensor. The correlation of biomarkers between blood and ISF is also in the spotlight. In spite of the correlation between levels of biomarkers and proteins in blood and ISF, the lagging time it takes to reach the equilibrium of analyte distribution in a human physiological system remains an interesting question. This concern directly affects the response time of the microneedle-based biosensor that detects the analyte information from the ISF.

Currently, just a few microneedle-based biosensors are commercially available on the market. The "FreeStyle Libre 14 days" device offers the coin-sized and thick microneedle-based biosensor that could conveniently attach to patient's skin while monitoring glucose for 14 days continuously [88, 126, 155]. The Dexcom G6 also provides continuous glucose monitoring system; the detection patch is attached to the skin for up to 10 days [88, 126, 155]. Both devices contain the detecting and monitoring parts wirelessly. The glucose results could be displayed on the mobile apps. Moreover, the Dexcom G6 contains a cloud system that could monitor the results remotely. The K'Watch is another continuous glucose monitoring device, which contains a micro-point patch sensor attached under the watch structure for monitoring glucose and lactate. The K'Watch contains a display monitor like the other common smartwatches that could easily access [184].

Many microneedle-based biosensors focus on development to achieve high performance of biosensors. However, microneedle-based biosensors aim to facilitate use and maximize benefits for medical management as well. To achieve this goal, integrations with other technologies are introduced. Integration of microneedle-based biosensors with smart devices [13, 185] and Internet of things (IoTs) can help microneedle-based biosensors to be accessible anywhere, anytime, and any devices. Furthermore, a minimally invasive sensor can collect information that can be analyzed to aid medical organizations in preventing and managing diseases in the community. Additionally, the real-time detection capabilities of microneedle-based biosensors can be integrated with drug delivery technology so that a closed-loop device can both detect biomarkers and provide personalized feedback of medications, such as the close loop of glucose and insulin. [186–188]. All of these potentials above could open up a new era of medical biosensing that minimizes healthcare costs and maximizes quality of life through easily and convenient approaches by using microneedle-based devices.

Acknowledgements We would like to thank the Talent Management Project of Prince of Songkla University. We also gratefully acknowledge the Center of Excellence for Innovation in Chemistry (PERCH-CIC), Ministry of Higher Education, Science, Research, and Innovation (MHESI).

Funding H.A. received MSc scholarship from the Faculty of Medicine and the Graduate School, Prince of Songkla University, Thailand. T.P. received support from the Sci-Pharm-Med Clustering Program Fund, Prince of Songkla University and the Office of the Permanent Secretary, Ministry of Higher Education, Science, Research, and Innovation (OPS MHESI), Thailand Science Research and Innovation (TSRI) (Grant No. RGNS63-230). I.J. received the support from National Research Council of Thailand (NRCT, Grant No. N41A640129), Prince of Songkla University, Hat Yai, Thailand.

Declarations

Conflict of interest The authors declare no competing interests.

References

1. Chinnadayyala SR, Cho S (2020) Porous platinum black-coated minimally invasive microneedles for non-enzymatic continuous glucose monitoring in interstitial fluid. Nanomaterials 11:37. https://doi.org/10.3390/nano11010037
2. Cass AEG, Sharma S, Microneedle enzyme sensor arrays for continuous in vivo monitoring, in Methods in enzymology. 2017, Elsevier Inc. pp. 413–427.
3. Cappon G, Vettoretti M, Sparacino G, Facchinetti A (2019) Continuous glucose monitoring sensors for diabetes management: a review of technologies and applications. Diabetes Metab J 43:383. https://doi.org/10.4093/dmj.2019.0121
4. El-Laboudi A, Oliver NS, Cass A, Johnston D (2013) Use of microneedle array devices for continuous glucose monitoring: a review, in Diabetes Technology and Therapeutics. Mary Ann Liebert, Inc. 140 Huguenot Street, 3rd Floor New Rochelle, NY 10801 USA. pp. 101–115
5. Heikenfeld J, Jajack A, Feldman B, Granger SW, Gaitonde S, Begtrup G, Katchman BA (2019) Accessing analytes in biofluids for peripheral biochemical monitoring. Nat Biotechnol 37:407–419. https://doi.org/10.1038/s41587-019-0040-3
6. Kim KB, Lee W-C, Cho C-H, Park D-S, Cho SJ, Shim Y-B (2019) Continuous glucose monitoring using a microneedle array sensor coupled with a wireless signal transmitter. Sensors Actuators B: Chem 281:14–21. https://doi.org/10.1016/j.snb.2018.10.081
7. Klonoff DC, Ahn D, Drincic A (2017) Continuous glucose monitoring: a review of the technology and clinical use. Diabetes Res Clin Pract 133:178–192. https://doi.org/10.1016/j.diabres.2017.08.005
8. Lee I, Probst D, Klonoff D, Sode K (2021) Continuous glucose monitoring systems - current status and future perspectives of the flagship technologies in biosensor research. Biosens Bioelectron 181:113054. https://doi.org/10.1016/j.bios.2021.113054
9. Bollella P, Sharma S, Cass AEG, Antiochia R (2019) Microneedle-based biosensor for minimally-invasive lactate detection. Biosens Bioelectron 123:152–159. https://doi.org/10.1016/j.bios.2018.08.010
10. Bollella P, Sharma S, Cass AEG, Antiochia R (2019) Minimally-invasive microneedle-based biosensor array for simultaneous lactate and glucose monitoring in artificial interstitial fluid. Electroanalysis 31:374–382. https://doi.org/10.1002/elan.201800630
11. Rathee K, Dhull V, Dhull R, Singh S (2016) Biosensors based on electrochemical lactate detection: a comprehensive review. Biochem Biophys Rep 5:35–54. https://doi.org/10.1016/j.bbrep.2015.11.010
12. Sharma S, Saeed A, Johnson C, Gadegaard N, Cass AE (2017) Rapid, low cost prototyping of transdermal devices for personal healthcare monitoring. In: Sensing and Bio-Sensing Research. Elsevier B.V., pp 104–108. https://doi.org/10.1016/j.sbsr.2016.10.004
13. Tehrani F, Teymourian H, Wuerstle B, Kavner J, Patel R, Furmidge A, Aghavali R, Hosseini-Toudeshki H, Brown C, Zhang F, Mahato K, Li Z, Barfidokht A, Yin L, Warren P, Huang N, Patel Z, Mercier PP, Wang J (2022) An integrated wearable microneedle array for the continuous monitoring of multiple biomarkers in interstitial fluid. Nat Biomed Eng. https://doi.org/10.1038/s41551-022-00887-1
14. Teymourian H, Moonla C, Tehrani F, Vargas E, Aghavali R, Barfidokht A, Tangkuaram T, Mercier PP, Dassau E, Wang J (2020) Microneedle-based detection of ketone bodies along with glucose and lactate: toward real-time continuous interstitial fluid monitoring of diabetic ketosis and ketoacidosis. Anal Chem 92:2291–2300. https://doi.org/10.1021/acs.analchem.9b05109
15. Alba-Patino A, Vaquer A, Baron E, Russell SM, Borges M, de la Rica R (2022) Micro- and nanosensors for detecting blood pathogens and biomarkers at different points of sepsis care. Mikrochim Acta 189:74. https://doi.org/10.1007/s00604-022-05171-2
16. Booth MA, Gowers SAN, Leong CL, Rogers ML, Samper IC, Wickham AP, Boutelle MG (2018) Chemical monitoring in clinical settings: recent developments toward real-time chemical monitoring of patients. Anal Chem 90:2–18. https://doi.org/10.1021/acs.analchem.7b04224
17. Teymourian H, Tehrani F, Mahato K, Wang J (2021) Lab under the skin: microneedle based wearable devices. Adv Healthc Mater 10:2002255. https://doi.org/10.1002/adhm.202002255
18. Bhatnagar S, Gadeela PR, Thathireddy P, Venuganti VVK (2019) Microneedle-based drug delivery: materials of construction. J Chem Sci 1–28. https://doi.org/10.1007/s12039-019-1666-x
19. Rawson TM, Gowers SAN, Freeman DME, Wilson RC, Sharma S, Gilchrist M, Macgowan A, Lovering A, Bayliss M, Kyriakides M, Georgiou P, Cass AEG, O'Hare D, Holmes AH (2019) Microneedle biosensors for real-time, minimally invasive drug monitoring of phenoxymethylpenicillin: a first-in-human evaluation in healthy volunteers. Lancet Digital Health 1:e335–e343. https://doi.org/10.1016/s2589-7500(19)30131-1
20. Joyce JC, Carroll TD, Collins ML, Chen MH, Fritts L, Dutra JC, Rourke TL, Goodson JL, McChesney MB, Prausnitz MR, Rota PA (2018) A microneedle patch for measles and rubella vaccination is immunogenic and protective in infant rhesus macaques. J Infect Dis 218:124–132. https://doi.org/10.1093/infdis/jiy139
21. Sullivan SP, Koutsonanos DG, Del Pilar MM, Lee JW, Zarnitsyn V, Choi S-O, Murthy N, Compans RW, Skountzou I, Prausnitz MR (2010) Dissolving polymer microneedle patches for influenza vaccination. Nat Med 16:915–920. https://doi.org/10.1038/nm.2182
22. Donadei A, Kraan H, Ophorst O, Flynn O, O'Mahony C, Soema PC, Moore AC (2019) Skin delivery of trivalent Sabin inactivated poliovirus vaccine using dissolvable microneedle patches induces neutralizing antibodies. J Control Release 311–312:96–103. https://doi.org/10.1016/j.jconrel.2019.08.039
23. Goud KY, Moonla C, Mishra RK, Yu C, Narayan R, Litvan I, Wang J (2019) Wearable electrochemical microneedle sensor for continuous monitoring of levodopa: toward parkinson management. ACS Sens 4:2196–2204. https://doi.org/10.1021/acssensors.9b01127
24. Tasca F, Tortolini C, Bollella P, Antiochia R (2019) Microneedle-based electrochemical devices for transdermal biosensing: a review. Curr Opin Electrochem 16:42–49. https://doi.org/10.1016/j.coelec.2019.04.003
25. Lee C, Yang H, Kim S, Kim M, Kang H, Kim N, An S, Koh J, Jung H (2016) Evaluation of the anti-wrinkle effect of an ascorbic acid-loaded dissolving microneedle patch via a double-blind, placebo-controlled clinical study. Int J Cosmet Sci 38:375–381. https://doi.org/10.1111/ics.12299
26. Jang M, Baek S, Kang G, Yang H, Kim S, Jung H (2020) Dissolving microneedle with high molecular weight hyaluronic acid to improve skin wrinkles, dermal density and elasticity. Int J Cosmet Sci 42:302–309. https://doi.org/10.1111/ics.12617
27. Jang D, Shim J, Shin DM, Noh H, Oh SJ, Park JH, Lee JH (2022) Magnesium microneedle patches for under-eye wrinkles. Dermatol Ther 35:e15732. https://doi.org/10.1111/dth.15732
28. Pere CPP, Economidou SN, Lall G, Ziraud C, Boateng JS, Alexander BD, Lamprou DA, Douroumis D (2018) 3D printed

microneedles for insulin skin delivery. In: International Journal of Pharmaceutics. Elsevier, pp 425–432. https://doi.org/10.1016/j.ijpharm.2018.03.031
29. Chinnadayyala SR, Park KD, Cho S (2018) Editors' choice—review—in vivo and in vitro microneedle based enzymatic and non-enzymatic continuous glucose monitoring biosensors. ECS J Solid State Sci Technol 7:Q3159–Q3171. https://doi.org/10.1149/2.0241807jss
30. Zhang BL, Zhang XP, Chen BZ, Fei WM, Cui Y, Guo XD (2021) Microneedle-assisted technology for minimally invasive medical sensing. In: Microchemical Journal. Elsevier B.V., pp 105830. https://doi.org/10.1016/j.microc.2020.105830
31. Johnson AR, Procopio AT (2019) Low cost additive manufacturing of microneedle masters. In: 3D Printing in Medicine. 3D Printing in Medicine. https://doi.org/10.1186/s41205-019-0039-x
32. Khanna P, Luongo K, Strom JA, Bhansali S (2010) Sharpening of hollow silicon microneedles to reduce skin penetration force. J Micromech Microeng 20:045011. https://doi.org/10.1088/0960-1317/20/4/045011
33. Bonfante G, Lee H, Bao L, Park J, Takama N, Kim B (2020) Comparison of polymers to enhance mechanical properties of microneedles for bio-medical applications. Micro Nano Syst Lett 8https://doi.org/10.1186/s40486-020-00113-0
34. Du G, Zhang Z, He P, Zhang Z, Sun X (2021) Determination of the mechanical properties of polymeric microneedles by micromanipulation. J Mech Behav Biomed Mater 117:104384. https://doi.org/10.1016/j.jmbbm.2021.104384
35. Gittard SD, Chen B, Xu H, Ovsianikov A, Chichkov BN, Monteiro-Riviere NA, Narayan RJ (2013) The effects of geometry on skin penetration and failure of polymer microneedles. J Adhes Sci Technol 27:227–243. https://doi.org/10.1080/01694243.2012.705101
36. Dervisevic M, Alba M, Prieto-Simon B, Voelcker NH (2020) Skin in the diagnostics game: wearable biosensor nano- and microsystems for medical diagnostics. Nano Today 30:100828. https://doi.org/10.1016/j.nantod.2019.100828
37. Madden J, O'Mahony C, Thompson M, O'Riordan A, Galvin P (2020) Biosensing in dermal interstitial fluid using microneedle based electrochemical devices. Sens Bio-Sens Res 29:100348. https://doi.org/10.1016/j.sbsr.2020.100348
38. Ventrelli L, Strambini LM, Barillaro G (2015) Microneedles for transdermal biosensing: current picture and future direction. Adv Healthc Mater 4:2606–2640. https://doi.org/10.1002/adhm.201500450
39. Ribet F, Stemme G, Roxhed N (2018) Real-time intradermal continuous glucose monitoring using a minimally invasive microneedle-based system. Biomed Microdevices 20:101. https://doi.org/10.1007/s10544-018-0349-6
40. Dabbagh SR, Sarabi MR, Rahbarghazi R, Sokullu E, Yetisen AK, Tasoglu S (2021) 3D-printed microneedles in biomedical applications. Iscience 24:102012. https://doi.org/10.1016/j.isci.2020.102012
41. Gurjarpadhye AA (2011) Effect of localized mechanical indentation on skin water content evaluated using OCT. J Biomed Imaging 2011:17
42. Tobin DJ (2006) Biochemistry of human skin - our brain on the outside. Chem Soc Rev 35:52–67. https://doi.org/10.1039/b505793k
43. Wong R, Geyer S, Weninger W, Guimberteau JC, Wong JK (2016) The dynamic anatomy and patterning of skin. Exp Dermatol 25:92–98. https://doi.org/10.1111/exd.12832
44. Crichton ML, Chen X, Huang H, Kendall MAF (2013) Elastic modulus and viscoelastic properties of full thickness skin characterised at micro scales. Biomaterials 34:2087–2097. https://doi.org/10.1016/j.biomaterials.2012.11.035
45. Ligon SC, Liska R, Stampfl J, Gurr M, Mülhaupt R (2017) Polymers for 3D printing and customized additive manufacturing. Chem Rev 117:10212–10290
46. Evens T, Malek O, Castagne S, Seveno D, Van Bael A (2020) A novel method for producing solid polymer microneedles using laser ablated moulds in an injection moulding process. Manuf Lett 24:29–32. https://doi.org/10.1016/j.mfglet.2020.03.009
47. Romgens AM, Bader DL, Bouwstra JA, Baaijens FPT, Oomens CWJ (2014) Monitoring the penetration process of single microneedles with varying tip diameters. J Mech Behav Biomed Mater 40:397–405. https://doi.org/10.1016/j.jmbbm.2014.09.015
48. Davis SP, Landis BJ, Adams ZH, Allen MG, Prausnitz MR (2004) Insertion of microneedles into skin: measurement and prediction of insertion force and needle fracture force. J Biomech 37:1155–1163. https://doi.org/10.1016/j.jbiomech.2003.12.010
49. Park JH, Prausnitz MR (2010) Analysis of the mechanical failure of polymer microneedles by axial force. J Korean Phys Soc 56:1223–1227. https://doi.org/10.3938/jkps.56.1223
50. Gupta J, Park SS, Bondy B, Felner EI, Prausnitz MR (2011) Infusion pressure and pain during microneedle injection into skin of human subjects. Biomaterials 32:6823–6831. https://doi.org/10.1016/j.biomaterials.2011.05.061
51. Lee G, Ma Y, Lee Y-H, Jung H (2018) Clinical evaluation of a low-pain long microneedle for subcutaneous insulin injection. BioChip J 12:309–316. https://doi.org/10.1007/s13206-018-2411-0
52. Haq MI, Smith E, John DN, Kalavala M, Edwards C, Anstey A, Morrissey A, Birchall JC (2009) Clinical administration of microneedles: skin puncture, pain and sensation. Biomed Microdevices 11:35–47. https://doi.org/10.1007/s10544-008-9208-1
53. Miller PR, Taylor RM, Tran BQ, Boyd G, Glaros T, Chavez VH, Krishnakumar R, Sinha A, Poorey K, Williams KP, Branda SS, Baca JT, Polsky R (2018) Extraction and biomolecular analysis of dermal interstitial fluid collected with hollow microneedles. Commun Biol 1:173. https://doi.org/10.1038/s42003-018-0170-z
54. Gill HS, Denson DD, Burris BA, Prausnitz MR (2008) Effect of microneedle design on pain in human volunteers. Clin J Pain 585–594. https://doi.org/10.1097/ajp.0b013e31816778f9
55. Gill HS, Denson DD, Burris BA, Prausnitz MR (2008) Effect of microneedle design on pain in human volunteers. Clin J Pain 24:585–594. https://doi.org/10.1097/AJP.0b013e31816778f9
56. Han D, Morde RS, Mariani S, La Mattina AA, Vignali E, Yang C, Barillaro G, Lee H (2020) 4D printing of a bioinspired microneedle array with backward-facing barbs for enhanced tissue adhesion. Adv Funct Mater 30:1909197. https://doi.org/10.1002/adfm.201909197
57. Plamadeala C, Gosain SR, Hischen F, Buchroithner B, Puthukodan S, Jacak J, Bocchino A, Whelan D, O'Mahony C, Baumgartner W, Heitz J (2020) Bio-inspired microneedle design for efficient drug/vaccine coating. Biomed Microdevices 22https://doi.org/10.1007/s10544-019-0456-z
58. Trautmann A, Roth G-L, Nujiqi B, Walther T, Hellmann R (2019) Towards a versatile point-of-care system combining femtosecond laser generated microfluidic channels and direct laser written microneedle arrays. Microsyst Nanoeng 5https://doi.org/10.1038/s41378-019-0046-5
59. Yeung C, Chen S, King B, Lin H, King K, Akhtar F, Diaz G, Wang B, Zhu J, Sun W, Khademhosseini A, Emaminejad S (2019) A 3D-printed microfluidic-enabled hollow microneedle architecture for transdermal drug delivery. Biomicrofluidics 13:064125. https://doi.org/10.1063/1.5127778
60. Economidou SN, Uddin MJ, Marques MJ, Douroumis D, Sow WT, Li H, Reid A, Windmill JFC, Podoleanu A (2021) A novel 3D printed hollow microneedle microelectromechanical system for controlled, personalized transdermal drug delivery. Addit Manuf 38https://doi.org/10.1016/j.addma.2020.101815
61. Waghule T, Singhvi G, Dubey SK, Pandey MM, Gupta G, Singh M, Dua K (2019) Microneedles: a smart approach and increasing potential for transdermal drug delivery system. Biomed

Pharmacother 109:1249–1258. https://doi.org/10.1016/j.biopha.2018.10.078
62. Windmiller JR, Zhou N, Chuang M-C, Valdés-Ramírez G, Santhosh P, Miller PR, Narayan R, Wang J (2011) Microneedle array-based carbon paste amperometric sensors and biosensors. In: The Analyst. Royal Society of Chemistry, pp 1846. https://doi.org/10.1039/c1an00012h
63. Goud KY, Mahato K, Teymourian H, Longardner K, Litvan I, Wang J (2022) Wearable electrochemical microneedle sensing platform for real-time continuous interstitial fluid monitoring of apomorphine: toward Parkinson management. Sensors Actuators B Chem 354https://doi.org/10.1016/j.snb.2021.131234
64. Han D, Morde RS, Mariani S, La Mattina AA, Vignali E, Yang C, Barillaro G, Lee H (2020) 4D printing of a bioinspired microneedle array with backward-facing barbs for enhanced tissue adhesion. Adv Funct Mater 30:1909197. https://doi.org/10.1002/adfm.201909197
65. Gao J, Huang W, Chen Z, Yi C, Jiang L (2019) Simultaneous detection of glucose, uric acid and cholesterol using flexible microneedle electrode array-based biosensor and multi-channel portable electrochemical analyzer. Sensors Actuators B Chem 287:102–110 https://doi.org/10.1016/j.snb.2019.02.020
66. Jeerapan I, Poorahong S (2020) Review—flexible and stretchable electrochemical sensing systems: materials, energy sources, and integrations. J Electrochem Soc 167:037573. https://doi.org/10.1149/1945-7111/ab7117
67. Bader D, Bowker P (1983) Mechanical characteristics of skin and underlying tissues in vivo. Biomaterials 4:305–308
68. Mostafavi Yazdi SJ, Baqersad J (2022) Mechanical modeling and characterization of human skin: a review. J Biomech 130:110864. https://doi.org/10.1016/j.jbiomech.2021.110864
69. Everett JS, Sommers MS (2013) Skin viscoelasticity: physiologic mechanisms, measurement issues, and application to nursing science. Biol Res Nurs 15:338–346. https://doi.org/10.1177/1099800411434151
70. Jacquemoud C, Bruyere-Garnier K, Coret M (2007) Methodology to determine failure characteristics of planar soft tissues using a dynamic tensile test. J Biomech 40:468–475. https://doi.org/10.1016/j.jbiomech.2005.12.010
71. Sebastia-Saez D, Benaouda F, Lim CH, Lian G, Jones S, Chen T, Cui L (2021) Numerical analysis of the strain distribution in skin domes formed upon the application of hypobaric pressure. Skin Res Technol 27:948–958. https://doi.org/10.1111/srt.13047
72. Salter D, McArthur H, Crosse J, Dickens A (1993) Skin mechanics measured in vivo using torsion: a new and accurate model more sensitive to age, sex and moisturizing treatment. Int J Cosmetic Sci 15:200–218
73. Sanders R (1973) Torsional elasticity of human skin in vivo. Pflugers Arch 342:255–260. https://doi.org/10.1007/BF00591373
74. Groves RB, Coulman SA, Birchall JC, Evans SL (2012) Quantifying the mechanical properties of human skin to optimise future microneedle device design. Comput Methods Biomech Biomed Eng 15:73–82. https://doi.org/10.1080/10255842.2011.596481
75. Anastasova S, Crewther B, Bembnowicz P, Curto V, Ip HMD, Rosa B, Yang G-Z (2017) A wearable multisensing patch for continuous sweat monitoring. Biosens Bioelectron 93:139–145 https://doi.org/10.1016/j.bios.2016.09.038
76. Pailler-Mattei C, Bec S, Zahouani H (2008) In vivo measurements of the elastic mechanical properties of human skin by indentation tests. Med Eng Phys 30:599–606. https://doi.org/10.1016/j.medengphy.2007.06.011
77. Ranamukhaarachchi SA, Lehnert S, Ranamukhaarachchi SL, Sprenger L, Schneider T, Mansoor I, Rai K, Häfeli UO, Stoeber B (2016) A micromechanical comparison of human and porcine skin before and after preservation by freezing for medical device development. Sci Rep 6:32074. https://doi.org/10.1038/srep32074
78. Widianto DP, Stewart BG, Mena-Lapaix JL, Shafer RH, Burns A, Prausnitz MR, Alizadeh A, Sitaraman SK (2021) Microneedle insertion into visco-hyperelastic model for skin for healthcare application. In: 2021 IEEE 71st Electronic Components and Technology Conference (ECTC). IEEE. https://doi.org/10.1109/ECTC32696.2021.00236
79. Park S, Kim M, Baek S-K, Park J-H, Choi S-O (2019) Spray-formed layered polymer microneedles for controlled biphasic drug delivery. Polymers 11:369. https://doi.org/10.3390/polym11020369
80. Krieger KJ, Bertollo N, Dangol M, Sheridan JT, Lowery MM, O'Cearbhaill ED (2019) Simple and customizable method for fabrication of high-aspect ratio microneedle molds using low-cost 3D printing. Microsyst Nanoeng 5:42. https://doi.org/10.1038/s41378-019-0088-8
81. Zheng M, Wang Z, Chang H, Wang L, Chew SWT, Lio DCS, Cui M, Liu L, Tee BCK, Xu C (2020) Osmosis-powered hydrogel microneedles for microliters of skin interstitial fluid extraction within minutes. Adv Healthc Mater 9:1901683. https://doi.org/10.1002/adhm.201901683
82. Cho I-H, Kim DH, Park S (2020) Electrochemical biosensors: perspective on functional nanomaterials for on-site analysis. Biomater Res 24https://doi.org/10.1186/s40824-019-0181-y
83. Abdulbari HA, Basheer EAM (2017) Electrochemical biosensors: electrode development, materials, design, and fabrication. ChemBioEng Rev 4:92–105. https://doi.org/10.1002/cben.201600009
84. Freire RS, Pessoa CA, Mello LD, Kubota LT (2003) Direct electron transfer: an approach for electrochemical biosensors with higher selectivity and sensitivity. J Braz Chem Soc 14:230–243. https://doi.org/10.1590/s0103-50532003000200008
85. Bartlett PN, Al-Lolage FA (2018) There is no evidence to support literature claims of direct electron transfer (DET) for native glucose oxidase (GOx) at carbon nanotubes or graphene. J Electroanal Chem 819:26–37. https://doi.org/10.1016/j.jelechem.2017.06.021
86. Chodankar NR, Pham HD, Nanjundan AK, Fernando JFS, Jayaramulu K, Golberg D, Han YK, Dubal DP (2020) True meaning of pseudocapacitors and their performance metrics: asymmetric versus hybrid supercapacitors. Small 16:e2002806. https://doi.org/10.1002/smll.202002806
87. Ma G, Wu C (2017) Microneedle, bio-microneedle and bio-inspired microneedle: a review. J Control Release 251:11–23. https://doi.org/10.1016/j.jconrel.2017.02.011
88. Liu Y, Yu Q, Luo X, Yang L, Cui Y (2021) Continuous monitoring of diabetes with an integrated microneedle biosensing device through 3D printing. Microsyst Nanoeng 7https://doi.org/10.1038/s41378-021-00302-w
89. Zhang BL, Yang Y, Zhao ZQ, Guo XD (2020) A gold nanoparticles deposited polymer microneedle enzymatic biosensor for glucose sensing. Electrochim Acta 358:136917
90. Kai H, Kumatani A (2021) A porous microneedle electrochemical glucose sensor fabricated on a scaffold of a polymer monolith. J Phys Energy 3:024006. https://doi.org/10.1088/2515-7655/abe4a1
91. Lee H, Bonfante G, Sasaki Y, Takama N, Minami T, Kim B (2020) Porous microneedles on a paper for screening test of prediabetes. Med Dev Sensors 3https://doi.org/10.1002/mds3.10109
92. Triroj N, Saensak R, Porntheeraphat S, Paosawatyanyong B, Amornkitbamrung V (2020) Diamond-like carbon thin film electrodes for microfluidic bioelectrochemical sensing platforms. Anal Chem 92:3650–3657. https://doi.org/10.1021/acs.analchem.9b04689

93. Cho IH, Kim DH, Park S (2020) Electrochemical biosensors: perspective on functional nanomaterials for on-site analysis. Biomater Res 24:6. https://doi.org/10.1186/s40824-019-0181-y
94. Taniselass S, Arshad MKM, Gopinath SCB (2019) Graphene-based electrochemical biosensors for monitoring noncommunicable disease biomarkers. Biosens Bioelectron 130:276–292. https://doi.org/10.1016/j.bios.2019.01.047
95. Joshi P, Mishra R, Narayan RJ (2021) Biosensing applications of carbon-based materials. Curr Opin Biomed Eng 18:100274. https://doi.org/10.1016/j.cobme.2021.100274
96. Jeerapan, Ma (2019) Challenges and opportunities of carbon nanomaterials for biofuel cells and supercapacitors: personalized energy for futuristic self-sustainable devices. C — J Carbon Res 5:62 https://doi.org/10.3390/c5040062
97. Jin Q, Chen H-J, Li X, Huang X, Wu Q, He G, Hang T, Yang C, Jiang Z, Li E, Zhang A, Lin Z, Liu F, Xie X (2019) Reduced graphene oxide nanohybrid-assembled microneedles as minimally invasive electrodes for real-time transdermal biosensing. Small 15:1804298. https://doi.org/10.1002/smll.201804298
98. Kazemi SH, Ghodsi E, Abdollahi S, Nadri S (2016) Porous graphene oxide nanostructure as an excellent scaffold for label-free electrochemical biosensor: detection of cardiac troponin I. Mater Sci Eng C 69:447–452. https://doi.org/10.1016/j.msec.2016.07.005
99. Yun YS, Yoon G, Park M, Cho SY, Lim H-D, Kim H, Park YW, Kim BH, Kang K, Jin H-J (2016) Restoration of thermally reduced graphene oxide by atomic-level selenium doping. NPG Asia Mater 8:e338–e338. https://doi.org/10.1038/am.2016.191
100. Mao HY, Laurent S, Chen W, Akhavan O, Imani M, Ashkarran AA, Mahmoudi M (2013) Graphene: promises, facts, opportunities, and challenges in nanomedicine. Chem Rev 113:3407–3424. https://doi.org/10.1021/cr300335p
101. Sur UK (2012) Graphene: a rising star on the horizon of materials science. Int J Electrochem 2012:1–12. https://doi.org/10.1155/2012/237689
102. Geim AK, Novoselov KS (2007) The rise of graphene. Nat Mater 6:183–191. https://doi.org/10.1038/nmat1849
103. Heydari-Bafrooei E, Ensafi AA (2019) Chapter 4 - typically used carbon-based nanomaterials in the fabrication of biosensors. In: Ensafi AA (ed) Electrochemical biosensors. Elsevier, pp 77–98. https://doi.org/10.1016/B978-0-12-816491-4.00004-8
104. Benchirouf A, Müller C, Kanoun O (2016) Electromechanical behavior of chemically reduced graphene oxide and multi-walled carbon nanotube hybrid material. Nanoscale Res Lett 11https://doi.org/10.1186/s11671-015-1216-5
105. Yang W, Ratinac KR, Ringer SP, Thordarson P, Gooding JJ, Braet F (2010) Carbon nanomaterials in biosensors: should you use nanotubes or graphene? Angew Chem Int Ed 49:2114–2138. https://doi.org/10.1002/anie.200903463
106. Wijeratne K, Ail U, Brooke R, Vagin M, Liu X, Fahlman M, Crispin X (2018) Bulk electronic transport impacts on electron transfer at conducting polymer electrode–electrolyte interfaces. In: Proceedings of the National Academy of Sciences of the United States of America, pp 11899–11904. https://doi.org/10.1073/pnas.1806087115
107. Liu M, Wen Y, Xu J, He H, Li D, Yue R, Liu G (2011) An amperometric biosensor based on ascorbate oxidase immobilized in poly(3,4-ethylenedioxythiophene)/multi-walled carbon nanotubes composite films for the determination of l-ascorbic acid. In: Analytical Sciences, pp 477–482. https://doi.org/10.2116/analsci.27.477
108. Teles FRR, Fonseca LP (2008) Applications of polymers for biomolecule immobilization in electrochemical biosensors. Mater Sci Eng C 28:1530–1543. https://doi.org/10.1016/j.msec.2008.04.010
109. Li J, Lin X (2007) Simultaneous determination of dopamine and serotonin on gold nanocluster/overoxidized-polypyrrole composite modified glassy carbon electrode. Sensors Actuators B Chem 124:486–493. https://doi.org/10.1016/j.snb.2007.01.021
110. Yoon Y, Lee GS, Yoo K, Lee JB (2013) Fabrication of a microneedle/CNT hierarchical micro/nano surface electrochemical sensor and its in-vitro glucose sensing characterization. Sensors (Basel) 13:16672–16681. https://doi.org/10.3390/s131216672
111. Skaria E, Patel BA, Flint MS, Ng KW (2019) Poly(lactic acid)/carbon nanotube composite microneedle arrays for dermal biosensing. Anal Chem 91:4436–4443. https://doi.org/10.1021/acs.analchem.8b04980
112. Li X, Huang X, Mo J, Wang H, Huang Q, Yang C, Zhang T, Chen HJ, Hang T, Liu F, Jiang L, Wu Q, Li H, Hu N, Xie X (2021) A fully integrated closed-loop system based on mesoporous microneedles-iontophoresis for diabetes treatment. Adv Sci 8:2100827. https://doi.org/10.1002/advs.202100827
113. Liu L, Kai H, Nagamine K, Ogawa Y, Nishizawa M (2016) Porous polymer microneedles with interconnecting microchannels for rapid fluid transport. RSC Adv 6:48630–48635. https://doi.org/10.1039/c6ra07882f
114. Roosterman D, Goerge T, Schneider SW, Bunnett NW, Steinhoff M (2006) Neuronal control of skin function: the skin as a neuroimmunoendocrine organ. Physiol Rev 86:1309–1379. https://doi.org/10.1152/physrev.00026.2005
115. Madhurantakam S, Karnam JB, Brabazon D, Takai M, Ahad IU, Balaguru Rayappan JB, Krishnan UM (2020) "Nano": an emerging avenue in electrochemical detection of neurotransmitters. ACS Chem Neurosci 11:4024–4047. https://doi.org/10.1021/acschemneuro.0c00355
116. Tortolini C, Cass AEG, Pofi R, Lenzi A, Antiochia R (2022) Microneedle-based nanoporous gold electrochemical sensor for real-time catecholamine detection. Mikrochim Acta 189:180. https://doi.org/10.1007/s00604-022-05260-2
117. Chinnadayyala SR, Park I, Cho S (2018) Nonenzymatic determination of glucose at near neutral pH values based on the use of nafion and platinum black coated microneedle electrode array. Mikrochim Acta 185:250. https://doi.org/10.1007/s00604-018-2770-1
118. Teodorescu M, Bercea M (2015) Poly(vinylpyrrolidone) – a versatile polymer for biomedical and beyond medical applications. Polym-Plast Technol Eng 54:923–943. https://doi.org/10.1080/03602559.2014.979506
119. Liu F, Lin Z, Jin Q, Wu Q, Yang C, Chen H-J, Cao Z, Lin D-A, Zhou L, Hang T, He G, Xu Y, Xia W, Tao J, Xie X (2019) Protection of nanostructures-integrated microneedle biosensor using dissolvable polymer coating. ACS Appl Mater Interfaces 11:4809–4819. https://doi.org/10.1021/acsami.8b18981
120. Musameh M, Wang J (2008) Sensitive and stable amperometric measurements at ionic liquid-carbon paste microelectrodes. Anal Chim Acta 606:45–49. https://doi.org/10.1016/j.aca.2007.11.012
121. Teymourian H, Salimi A, Hallaj R (2012) Electrocatalytic oxidation of NADH at electrogenerated NAD+ oxidation product immobilized onto multiwalled carbon nanotubes/ionic liquid nanocomposite: application to ethanol biosensing. Talanta 90:91–98. https://doi.org/10.1016/j.talanta.2012.01.003
122. Goud KY, Moonla C, Mishra RK, Yu C, Narayan R, Litvan I, Wang J (2019) Wearable electrochemical microneedle sensor for continuous monitoring of levodopa: toward parkinson management. ACS Sensors 4:2196–2204. https://doi.org/10.1021/acssensors.9b01127
123. Ng KW, Lau WM, Williams AC (2015) Towards pain-free diagnosis of skin diseases through multiplexed microneedles: biomarker extraction and detection using a highly sensitive blotting method. Drug Deliv Transl Res 5:387–396. https://doi.org/10.1007/s13346-015-0231-5
124. Coffey JW, Corrie SR, Kendall MA (2013) Early circulating biomarker detection using a wearable microprojection array skin

patch. Biomaterials 34:9572–9583. https://doi.org/10.1016/j.biomaterials.2013.08.078
125. Totti S, Ng KW, Dale L, Lian G, Chen T, Velliou EG (2019) A novel versatile animal-free 3D tool for rapid low-cost assessment of immunodiagnostic microneedles. Sensors Actuators B Chem 296. https://doi.org/10.1016/j.snb.2019.126652
126. Park M, Heo YJ (2021) Biosensing technologies for chronic diseases. BioChip J 15:1–13. https://doi.org/10.1007/s13206-021-00014-3
127. Nano A, Furst AL, Hill MG, Barton JK (2021) DNA electrochemistry: charge-transport pathways through DNA films on gold. J Am Chem Soc 143:11631–11640. https://doi.org/10.1021/jacs.1c04713
128. Benvidi A, Firouzabadi AD, Moshtaghiun SM, Mazloum-Ardakani M, Tezerjani MD (2015) Ultrasensitive DNA sensor based on gold nanoparticles/reduced graphene oxide/glassy carbon electrode. Anal Biochem 484:24–30. https://doi.org/10.1016/j.ab.2015.05.009
129. Evtugyn G, Porfireva A, Stepanova V, Budnikov H (2015) Electrochemical biosensors based on native DNA and nanosized mediator for the detection of anthracycline preparations. Electroanalysis 27:629–637. https://doi.org/10.1002/elan.201400564
130. Ensafi AA, Amini M, Rezaei B (2013) Detection of DNA damage induced by chromium/glutathione/H2O2 system at MWCNTs–poly(diallyldimethylammonium chloride) modified pencil graphite electrode using methylene blue as an electroactive probe. Sensors Actuators B Chem 177:862–870. https://doi.org/10.1016/j.snb.2012.12.017
131. Batasheva S, Fakhrullin R (2021) Sequence does not matter: the biomedical applications of DNA-based coatings and cores. Int J Mol Sci 22https://doi.org/10.3390/ijms222312884
132. Nguyen HH, Lee SH, Lee UJ, Fermin CD, Kim M (2019) Immobilized enzymes in biosensor applications. Materials 12:121. https://doi.org/10.3390/ma12010121
133. Song M, Lin X, Peng Z, Xu S, Jin L, Zheng X, Luo H (2021) Materials and methods of biosensor interfaces with stability. Front Mater 7https://doi.org/10.3389/fmats.2020.583739
134. Jesionowski T, Zdarta J, Krajewska B (2014) Enzyme immobilization by adsorption: a review. Adsorption 20:801–821. https://doi.org/10.1007/s10450-014-9623-y
135. Mohamad NR, Marzuki NH, Buang NA, Huyop F, Wahab RA (2015) An overview of technologies for immobilization of enzymes and surface analysis techniques for immobilized enzymes. Biotechnol Biotechnol Equip 29:205–220. https://doi.org/10.1080/13102818.2015.1008192
136. Chakraborty S, Rusli H, Nath A, Sikder J, Bhattacharjee C, Curcio S, Drioli E (2016) Immobilized biocatalytic process development and potential application in membrane separation: a review. Crit Rev Biotechnol 36:43–58. https://doi.org/10.3109/07388551.2014.923373
137. Homaei AA, Sariri R, Vianello F, Stevanato R (2013) Enzyme immobilization: an update. J Chem Biol 6:185–205. https://doi.org/10.1007/s12154-013-0102-9
138. Hassan ME, Yang Q, Xiao Z (2019) Covalent immobilization of glucoamylase enzyme onto chemically activated surface of κ-carrageenan. Bull Natl Res Cent 43https://doi.org/10.1186/s42269-019-0148-0
139. Martinkova P (2017) Main streams in the construction of biosensors and their applications. Int J Electrochem Sci 7386–7403 https://doi.org/10.20964/2017.08.02
140. Trevan M (1988) Enzyme immobilization by covalent bonding. In: New Protein Techniques. Springer, pp 495–510. https://doi.org/10.1385/0-89603-126-8:495
141. Smith S, Goodge K, Delaney M, Struzyk A, Tansey N, Frey M (2020) A comprehensive review of the covalent immobilization of biomolecules onto electrospun nanofibers. Nanomaterials (Basel) 10https://doi.org/10.3390/nano10112142
142. Dervisevic M, Alba M, Yan L, Senel M, Gengenbach TR, Prieto-Simon B, Voelcker NH (2022) Transdermal electrochemical monitoring of glucose via high-density silicon microneedle array patch. Adv Funct Mater 32:2009850. https://doi.org/10.1002/adfm.202009850
143. Dervisevic M, Alba M, Adams TE, Prieto-Simon B, Voelcker NH (2021) Electrochemical immunosensor for breast cancer biomarker detection using high-density silicon microneedle array. Biosens Bioelectron 192:113496. https://doi.org/10.1016/j.bios.2021.113496
144. Cannella V, Altomare R, Chiaramonte G, Di Bella S, Mira F, Russotto L, Pisano P, Guercio A (2019) Cytotoxicity evaluation of endodontic pins on L929 cell line. Biomed Res Int 2019:1–5. https://doi.org/10.1155/2019/3469525
145. Vidal MNP, Granjeiro JM (2017) Cytotoxicity tests for evaluating medical devices: an alert for the development of biotechnology health products. J Biomed Sci Eng 10:431–443. https://doi.org/10.4236/jbise.2017.109033
146. Li W, Zhou J, Xu Y (2015) Study of the in vitro cytotoxicity testing of medical devices. Biomed Rep 3:617–620. https://doi.org/10.3892/br.2015.481
147. Schossleitner K, O'Mahony C, Brandstatter S, Haslinger MJ, Demuth S, Fechtig D, Petzelbauer P (2019) Differences in biocompatibility of microneedles from cyclic olefin polymers with human endothelial and epithelial skin cells. J Biomed Mater Res A 107:505–512. https://doi.org/10.1002/jbm.a.36565
148. Yang B, Fang X, Kong J (2019) In situ sampling and monitoring cell-free DNA of the Epstein-Barr virus from dermal interstitial fluid using wearable microneedle patches. ACS Appl Mater Interfaces 11:38448–38458. https://doi.org/10.1021/acsami.9b12244
149. Johnson AR, Caudill CL, Tumbleston JR, Bloomquist CJ, Moga KA, Ermoshkin A, Shirvanyants D, Mecham SJ, Luft JC, DeSimone JM (2016) Single-step fabrication of computationally designed microneedles by continuous liquid interface production. In: Yamamoto M (ed) PLOS ONE. Public Library of Science, pp e0162518. https://doi.org/10.1371/journal.pone.0162518
150. da Silva AC, Córdoba de Torresi SI (2019) Advances in conducting, biodegradable and biocompatible copolymers for biomedical applications. In: Frontiers in Materials. Frontiers Media S.A., pp 98. https://doi.org/10.3389/fmats.2019.00098
151. Vicente-Perez EM, Larrañeta E, Mccrudden MTC, Kissenpfennig A, Hegarty S, Mccarthy HO, Donnelly RF (2017) Repeat application of microneedles does not alter skin appearance or barrier function and causes no measurable disturbance of serum biomarkers of infection, inflammation or immunity in mice in vivo. Eur J Pharm Biopharm 117:400–407. https://doi.org/10.1016/j.ejpb.2017.04.029
152. Lee Y-H, Chuang S-M, Huang S-C, Tan X, Liang R-Y, Yang GCC, Chueh PJ (2017) Biocompatibility assessment of nanomaterials for environmental safety screening. Environ Toxicol 32:1170–1182. https://doi.org/10.1002/tox.22313
153. Rodbard D (2016) Continuous glucose monitoring: a review of successes, challenges, and opportunities. Diabetes Technol Ther 18(Suppl 2):S3–S13. https://doi.org/10.1089/dia.2015.0417
154. Johnston L, Wang G, Hu K, Qian C, Liu G (2021) Advances in biosensors for continuous glucose monitoring towards wearables. Front Bioeng Biotechnol 9:733810. https://doi.org/10.3389/fbioe.2021.733810
155. Xue Y, Thalmayer AS, Zeising S, Fischer G, Lubke M (2022) Commercial and scientific solutions for blood glucose monitoring-a review. Sensors (Basel) 22https://doi.org/10.3390/s22020425

156. Misra S, Oliver NS (2015) Utility of ketone measurement in the prevention, diagnosis and management of diabetic ketoacidosis. Diabet Med 32:14–23. https://doi.org/10.1111/dme.12604
157. Federici MO, Benedetti MM (2006) Ketone bodies monitoring. Diabetes Res Clin Pract 74:S77–S81. https://doi.org/10.1016/s0168-8227(06)70004-3
158. Guerci B, Benichou M, Floriot ML, Bohme P, Fougnot S, Franck P, Drouin P (2003) Accuracy of an electrochemical sensor for measuring capillary blood ketones by fingerstick samples during metabolic deterioration after continuous subcutaneous insulin infusion interruption in type 1 diabetic patients. Diabetes Care 26:1137–1141. https://doi.org/10.2337/diacare.26.4.1137
159. Rimachi R, De Carvahlo FB, Orellano-Jimenez C, Cotton F, Vincent JL, De Backer D (2012) Lactate/pyruvate ratio as a marker of tissue hypoxia in circulatory and septic shock. Anaesth Intensive Care 40:427–432. https://doi.org/10.1177/0310057x1204000307
160. Luo TT, Sun ZH, Li CX, Feng JL, Xiao ZX, Li WD (2021) Monitor for lactate in perspiration. J Physiol Sci 71:26. https://doi.org/10.1186/s12576-021-00811-3
161. Alam F, RoyChoudhury S, Jalal AH, Umasankar Y, Forouzanfar S, Akter N, Bhansali S, Pala N (2018) Lactate biosensing: the emerging point-of-care and personal health monitoring. Biosens Bioelectron 117:818–829. https://doi.org/10.1016/j.bios.2018.06.054
162. Seshadri DR, Li RT, Voos JE, Rowbottom JR, Alfes CM, Zorman CA, Drummond CK (2019) Wearable sensors for monitoring the physiological and biochemical profile of the athlete. NPJ Digit Med 2:72. https://doi.org/10.1038/s41746-019-0150-9
163. Parrilla M, De Wael K (2021) Wearable self-powered electrochemical devices for continuous health management. Adv Funct Mater 31https://doi.org/10.1002/adfm.202107042
164. Mugo SM, Lu W, Lemieux S (2022) Stainless steel electrochemical capacitive microneedle sensors for multiplexed simultaneous measurement of pH, nitrates, and phosphates. Mikrochim Acta 189:206. https://doi.org/10.1007/s00604-022-05307-4
165. Chen L, Zhang C, Xiao J, You J, Zhang W, Liu Y, Xu L, Liu A, Xin H, Wang X (2020) Local extraction and detection of early stage breast cancers through a microneedle and nano-Ag/MBL film based painless and blood-free strategy. Mater Sci Eng C Mater Biol Appl 109:110402. https://doi.org/10.1016/j.msec.2019.110402
166. Song N, Xie P, Shen W, Oh H, Zhang Y, Vitale F, Javanmard M, Allen MG (2021) A microwell-based impedance sensor on an insertable microneedle for real-time in vivo cytokine detection. Microsyst Nanoeng 7:96. https://doi.org/10.1038/s41378-021-00297-4
167. Alimardani V, Abolmaali SS, Tamaddon AM, Ashfaq M (2021) Recent advances on microneedle arrays-mediated technology in cancer diagnosis and therapy. Drug Deliv Transl Res 11:788–816. https://doi.org/10.1007/s13346-020-00819-z
168. Keum DH, Jung HS, Wang T, Shin MH, Kim YE, Kim KH, Ahn GO, Hahn SK (2015) Microneedle biosensor for real-time electrical detection of nitric oxide for in situ cancer diagnosis during endomicroscopy. Adv Healthc Mater 4:1153–1158. https://doi.org/10.1002/adhm.201500012
169. Ciui B, Martin A, Mishra RK, Brunetti B, Nakagawa T, Dawkins TJ, Lyu M, Cristea C, Sandulescu R, Wang J (2018) Wearable wireless tyrosinase bandage and microneedle sensors: toward melanoma screening. Adv Healthc Mater 7:1701264. https://doi.org/10.1002/adhm.201701264
170. Hu Y, Li H, Li J (2018) A novel electrochemical biosensor for HIV-related DNA detection based on toehold strand displacement reaction and cruciform DNA crystal. J Electroanal Chem 822:66–72. https://doi.org/10.1016/j.jelechem.2018.05.011
171. Puttaswamy SV, Lubarsky GV, Kelsey C, Zhang X, Finlay D, Mclaughlin JA, Bhalla N (2020) Nanophotonic-carbohydrate lab-on-a-microneedle for rapid detection of human cystatin C in finger-prick blood. ACS Nano 14:11939–11949. https://doi.org/10.1021/acsnano.0c05074
172. Miller PR, Xiao X, Brener I, Burckel DB, Narayan R, Polsky R (2014) Microneedle-based transdermal sensor for on-chip potentiometric determination of K(+). Adv Healthc Mater 3:876–881. https://doi.org/10.1002/adhm.201300541
173. Gowers SAN, Freeman DME, Rawson TM, Rogers ML, Wilson RC, Holmes AH, Cass AE, O'Hare D (2019) Development of a minimally invasive microneedle-based sensor for continuous monitoring of beta-lactam antibiotic concentrations in vivo. ACS Sens 4:1072–1080. https://doi.org/10.1021/acssensors.9b00288
174. Mishra RK, Goud KY, Li Z, Moonla C, Mohamed MA, Tehrani F, Teymourian H, Wang J (2020) Continuous opioid monitoring along with nerve agents on a wearable microneedle sensor array. J Am Chem Soc 142:5991–5995. https://doi.org/10.1021/jacs.0c01883
175. Britch SC, Walsh SL (2022) Treatment of opioid overdose: current approaches and recent advances. Psychopharmacology 239:2063–2081. https://doi.org/10.1007/s00213-022-06125-5
176. Gerhard GS, Kaniper S, Paynton B (2020) Fentanyl overdoses and pharmacogenetics. Pharmacogenet Genomics 30:5–8. https://doi.org/10.1097/FPC.0000000000000389
177. De Deurwaerdere P, Di Giovanni G, Millan MJ (2017) Expanding the repertoire of L-DOPA's actions: a comprehensive review of its functional neurochemistry. Prog Neurobiol 151:57–100. https://doi.org/10.1016/j.pneurobio.2016.07.002
178. Lane EL (2019) L-DOPA for Parkinson's disease-a bittersweet pill. Eur J Neurosci 49:384–398. https://doi.org/10.1111/ejn.14119
179. Solis O, Moratalla R (2018) Dopamine receptors: homomeric and heteromeric complexes in L-DOPA-induced dyskinesia. J Neural Transm (Vienna) 125:1187–1194. https://doi.org/10.1007/s00702-018-1852-x
180. de la Fuente-Fernandez R, Sossi V, Huang Z, Furtado S, Lu JQ, Calne DB, Ruth TJ, Stoessl AJ (2004) Levodopa-induced changes in synaptic dopamine levels increase with progression of Parkinson's disease: implications for dyskinesias. Brain 127:2747–2754. https://doi.org/10.1093/brain/awh290
181. Sempionatto JR, Jeerapan I, Krishnan S, Wang J (2020) Wearable chemical sensors: emerging systems for on-body analytical chemistry. Anal Chem 92:378–396. https://doi.org/10.1021/acs.analchem.9b04668
182. Jeerapan I, Sonsa-ard T, Nacapricha D (2020) Applying nanomaterials to modern biomedical electrochemical detection of metabolites, electrolytes, and pathogens. Chemosensors 8https://doi.org/10.3390/chemosensors8030071
183. Kaur G, Kaur A, Kaur H (2021) Review on nanomaterials/conducting polymer based nanocomposites for the development of biosensors and electrochemical sensors. Polymer-Plastics Technology and Materials 60:504–521. https://doi.org/10.1080/25740881.2020.1844233
184. García-Guzmán JJ, Pérez-Ràfols C, Cuartero M, Crespo GA (2021) Microneedle based electrochemical (Bio)Sensing: towards decentralized and continuous health status monitoring. TrAC, Trends Anal Chem 135https://doi.org/10.1016/j.trac.2020.116148
185. Cheng Y, Gong X, Yang J, Zheng G, Zheng Y, Li Y, Xu Y, Nie G, Xie X, Chen M, Yi C, Jiang L (2022) A touch-actuated glucose sensor fully integrated with microneedle array and reverse iontophoresis for diabetes monitoring. Biosens Bioelectron 203:114026. https://doi.org/10.1016/j.bios.2022.114026

186. Bally L, Gubler P, Thabit H, Hartnell S, Ruan Y, Wilinska ME, Evans ML, Semmo M, Vogt B, Coll AP, Stettler C, Hovorka R (2019) Fully closed-loop insulin delivery improves glucose control of inpatients with type 2 diabetes receiving hemodialysis. Kidney Int 96:593–596. https://doi.org/10.1016/j.kint.2019.03.006
187. Boughton CK, Hovorka R (2021) New closed-loop insulin systems. Diabetologia 64:1007–1015. https://doi.org/10.1007/s00125-021-05391-w
188. Templer S (2022) Closed-loop insulin delivery systems: past, present, and future directions. Front Endocrinol (Lausanne) 13:919942. https://doi.org/10.3389/fendo.2022.919942